Asymptotic Methods

Carsten Henkel
Institut für Physik und Astronomie, Universität Potsdam

Preliminary lecture notes

November 2012

Presentation

This lecture is given with the aim to complement the undergraduate course in theoretical physics with a few approximation methods that are useful for calculations 'on paper'. The methods come under the name 'asymptotics' and allow to get approximate solutions to equations and integrals that one encounters in different fields of physics. The main idea is to identify small (or large) parameters and to make an expansion. This technique is a 'must' in physics, since exact solutions are the exception, not the rule. But approximations and expansions need also to be 'controlled' in the sense that one has to know how large are the errors one is making. Indeed, the difference between ordinary power series expansions (well-known in Taylor series, for example) and so-called asymptotic expansions is in the way errors and convergence are handled. We shall see that although the asymptotic series does not converge in the usual sense, it gives a better approximation than a conventional power series.

The general methods will be illustrated with examples from different fields of physics, with some emphasis on quantum mechanics. But similar techniques are also applied in hydrodynamics and optics.

From a historical perspective, asymptotic methods provide a way to recover a "simpler" description from a "more fundamental" one, for example classical mechanics from quantum mechanics. This point is quite paradigmatic for the structure of physical theories: e.g., we *know* that quantum mechanics is the more fundamental theory for the motion of material particles, but, nevertheless, classical mechanics is an excellent theory to describe the motion of planets, cars, or dust particles. It is thus a *limiting case* of the underlying quantum theory. In the same way, geometrical optics is a limiting case of wave optics, but accurate enough to engineer objects like telescopes, window panes, or contact lenses.

It is not easy to give a precise formulation of the limiting conditions under which geometrical optics is valid. A generally accepted way of speaking is:

'The optical wavelength λ is small compared to the other dimensions

of the problem.'[1]

For the mechanical theories, the formulation reads:

> 'The Planck constant $\hbar$ is small compared to the action of the corresponding classical system.'

These notes hopefully show in selected examples how these conditions acquire a sound mathematical sense.

Asymptotic approaches have been quite important for the discovery of quantum mechanics in the 1920s. The relation between geometrical and wave optics is at the very heart of E. SCHRÖDINGER's papers on his equation (1926a,1926b,1926c). In his interpretation, light rays and classical trajectories are identical concepts, and his equation is the strict analog of the wave equation of electrodynamics. In modern quantum mechanics courses, this intimate connection between classical and wave mechanics gets somewhat out of focus because the course also contains a lot of technical information about the algebraic formalism of quantum mechanics. This course tries to come back to the 'old-fashioned' wave mechanics and hopefully contributes to re-develop a small part of the intution people had when quantum mechanics was discovered. The focus will be on 'physics' and not on mathematical formalism.

There is still work being done in the field. Some of the examples presented in the lecture or as problems are coming from research papers that appeared no longer than ten years ago. Much can be learnt still about a quantum system by investigating the behaviour of the trajectories followed by its classical counterpart. 'Semiclassical' (or, perhaps better, 'semi-quantum') approximations thus allow to study the recent field of quantum chaos. Another example is particle optics. Electron, neutron and, more recently, atom beams have been used to perform optical experiments like reflection, diffraction, and interference. It is often the case that the particles' wavelength (the DE BROGLIE wavelength $\lambda = \hbar/mv$) is 'small', and semiclassical concepts are a powerful tool to describe the observations made in these experiments. Atom optics may even be considered as a test ground for wave mechanics because a large range of wavelengths (of energies) is available and the potentials may often be taylored at will, without dissipation and without strong interactions between the particles. A substantial number of problems given in this lecture are related to current experiments in that field. It often happens that the answer is not yet known, but may be expected within reasonable reach of semiclassical techniques.

[1] Throughout these notes, the 'reduced wavelength' $\lambda\!\!\!^{-} \equiv \lambda/2\pi$ is preferably used because the symbol looks so much like the (reduced) Planck constant $\hbar$.

Overview

The material of this lecture is grouped in three chapters:

1. the (J)WKB method in wave mechanics
2. asymptotic series and multiple-scale techniques for solving differential equations
3. caustics and quantum chaos (in two and three dimensions)

The **first chapter** does *not* stop with the standard WKB approximation of quantum mechanics textbooks. We also present uniform approximations developed by Berry and co-workers since 1970, that allow to find globally regular semiclassical wave functions (Berry & Mount, 1972). A large number of examples give the occasion to compare semiclassical and exact solutions. This has the additional benefit of providing insight into the asymptotics of special mathematical functions, as listed in Abramowitz & Stegun (1972); Gradshteyn & Ryzhik (1980), e.g. The chapter closes with a generalisation to two-component wave functions in one dimension: the Landau-Zener formula is derived.

The **second chapter** gives a more formal introduction into asymptotic series and how to identify singular points in differential equations. In this chapter, we illustrate the technique of 'matching' solutions to differential equations with small parameters that lead to a separation of length scales (Bender & Orszag, 1978; Nayfeh, 1981). This is known as the 'boundary layer problem' in hydrodynamics. It also provides a clean way to derive certain 'matching rules' that appear in the (J)WKB approximation.

In the **last chapter**, we move to more than one dimension and face the difficulty of generalizing the previous results. The opening example is the geometrical optics of the rainbow, and we go on to the fringe patterns that 'decorate' (Nye, 1999) the rainbow and other 'diffraction catastrophes' (Berry, 1981). The central paradigma developed is how to construct wave fronts with the help of light rays and what kind of interference phenomena happen near the 'natural focus' when this wave front is curved, also called a caustic. In the field of quantum chaos, classical rays or paths can be used to understand from a physical viewpoint the behaviour of the eigenfrequencies in a cavity or the energy spectrum in a box potential.

Bibliography

M. Abramowitz & I. A. Stegun, editors (1972). *Handbook of Mathematical Functions*. Dover Publications, Inc., New York, ninth edition.

C. M. Bender & S. A. Orszag (1978). *Advanced mathematical methods for scientists and engineers*. International series in pure and applied mathematics. McGraw-Hill Inc., New York.

M. V. Berry & K. E. Mount (1972). Semiclassical approximations in wave mechanics, *Rep. Prog. Phys.* **35**, 315–397.

M. V. Berry (1981). Singularities in Waves and Rays. in R. Balian & *al.*, editors, *Les Houches, Session XXXV, 1980*, pages 456–543. North Holland, Amsterdam.

I. S. Gradshteyn & I. M. Ryzhik (1980). *Table of Integrals, Series, and Products*. Academic Press Inc., San Diego.

A. H. Nayfeh (1981). *Introduction to Perturbation Techniques*. Wiley, New York.

J. F. Nye (1999). *Natural focusing and fine structure of light*. Institute of Physics Publishing, Bristol.

E. Schrödinger (1926a). Quantisierung als Eigenwertproblem. I, *Ann. Phys. (IV)* **79**, 361–376.

E. Schrödinger (1926b). Quantisierung als Eigenwertproblem. II, *Ann. Phys. (IV)* **79**, 489–527.

E. Schrödinger (1926c). Über das Verhältnis der Heisenberg–Born–Jordanschen Quantenmechanik zu der meinen, *Ann. Phys. (IV)* **79**, 734–756.

Chapter 1

(J)WKB method in wave mechanics

1.1 Motivation

We want to find an approximate solution to the stationary SCHRÖDINGER equation

$$-\frac{\hbar^2}{2m}\frac{\mathrm{d}^2}{\mathrm{d}x^2}\psi + V(x)\,\psi = E\psi(x) \tag{1.1}$$

in the limit where the Planck constant $\hbar$ is 'small'. Observe that it is not very useful to put $\hbar = 0$ in this equation because we do not have any differential equation any more (one talks of 'reducing the order' in the differential equation). In addition, we find that the wavefunction vanishes everywhere except at the classical turning points x_0 where $V(x_0) = E$.

A better solution is found following Schrödinger (1926): we make the following ansatz to the wave function

$$\psi(x) = A(x)\exp\left(\frac{\mathrm{i}}{\hbar}S(x)\right) \tag{1.2}$$

where the real function $S(x)$ has the dimension of an action. Putting (1.2) into the SCHRÖDINGER equation, we get

$$EA = \frac{1}{2m}\left(S'\right)^2 A + V(x)A \tag{1.3}$$

$$-\frac{\mathrm{i}\hbar}{2m}S''A - \frac{\mathrm{i}\hbar}{m}S'A' \tag{1.4}$$

$$-\frac{\hbar^2}{2m}A''$$

This equation already looks nicer when we put $\hbar = 0$:

$$\hbar \to 0: \quad \left(\frac{dS}{dx}\right)^2 = 2m(E - V(x)) \tag{1.5}$$

But we can do better and expand the action S in a power series

$$S = S_0 + \hbar S_1 + \dots \tag{1.6}$$

From (1.3,1.5), we clearly have the zeroth order solution

$$\begin{aligned} S_0(x) &= \pm \int^x \sqrt{2m\left(E - V(x')\right)}\,\mathrm{d}x' + \text{const.} && (1.7)\\ &= \pm \int^x p(x')\mathrm{d}x' + \text{const.} \\ p(x) &= \sqrt{2m\left(E - V(x)\right)} && (1.8) \end{aligned}$$

where $p(x)$ is the classical momentum for a particle moving to the right in the potential $V(x)$. The constant can be put into the starting point (lower boundary) of the integral.

The first order term (**??**) gives

$$\frac{S'}{m}\frac{\mathrm{d}A}{\mathrm{d}x} + \frac{A}{2m}S'' = 0, \tag{1.9}$$

and this may be integrated to give to lowest order in $\hbar$:

$$\frac{S_0'}{m}A^2 = \text{const} \quad \text{or} \quad A(x) = \frac{\text{const}}{\sqrt{p(x)}} \tag{1.10}$$

The constant can be interpreted as the probability current that is a conserved quantity in one dimension (for a stationary, time-independent probability density).

Stopping the expansion at this point, we get the following approximation to the wave function

$$\psi_{\mathrm{WKB}}(x) = \frac{C}{\sqrt{p(x)}} \exp\left(\pm\frac{\mathrm{i}}{\hbar}\int^x p(x')\mathrm{d}x'\right) \tag{1.11}$$

where the integration constants have been lumped into the global normalisation factor C. ψ_{WKB} is the wave function of the WENZEL KRAMERS BRILLOUIN approximation (Messiah, 1995), obtained already in the 1920's.

Classically allowed region

In one dimension, it is easy to distinguish two types of regions in configuration space (see fig.1.1): the 'classically allowed region' I (where $E > V(x)$) is accessible for a classical particle, while the region II ($E < V(x)$) is classically forbidden.

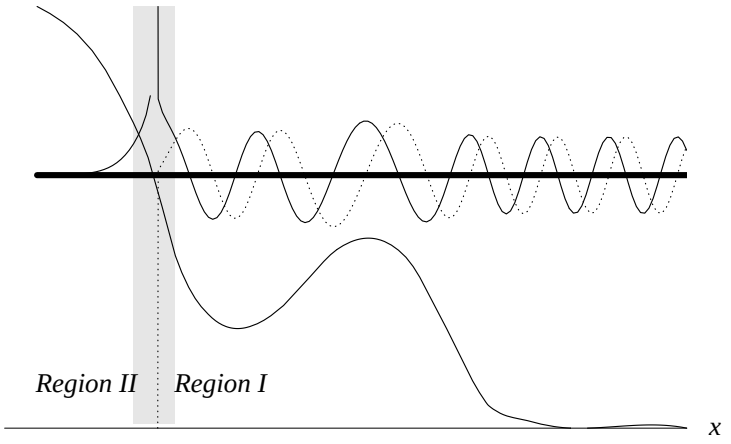

Figure 1.1: Classically allowed (I) and forbidden (II) regions for a particle of energy E in a potential $V(x)$. The thin solid and dotted lines show real and imaginary parts of the WKB wave function (1.11). The waves are not correctly matched at the transition point.

Consider in more detail the region I in fig.1.1. The momentum (1.8) is real there, and the WKB wave function (1.11) is the natural generalisation of a plane wave $\exp(\pm \mathrm{i}px/\hbar)$ that would propagate towards the right (left) if the momentum p were spatially constant (we conventionally use the factor $\exp(-\mathrm{i}Et/\hbar)$ for the time-dependence of the wave function). The wave function (1.11) being complex, we show its real and imaginary parts. They are oscillating and behave as $\cos\phi(x)$ and $\sin\phi(x)$ (sinusoidal curves with a phase difference $\pi/2$). From the relative positions of the maxima in the real and imaginary part, we deduce that the phase $\phi(x)$ increases towards the right, the figure thus shows a wave propagating to the right. In agreement with DE BROGLIE's formula $\lambda = \hbar/p$, the phase varies slowly (the wave length is large) when the classical momentum $p(x)$ is small (above the barrier in the figure), while it varies rapidly when $p(x)$ is larger.

As regards the envelope of the oscillations, it follows an opposite trend: the magnitude of the wave function $|\psi(x)| = C/\sqrt{p(x)}$ is larger when the particle moves more slowly. This is because the quantity $|\psi(x)|^2\mathrm{d}x = \rho(x)\mathrm{d}x$ gives the probability to find the particle in the interval $x \ldots x + \mathrm{d}x$. Since for a stationary flow in one dimension, the equation of continuity gives $\partial j/\partial x = -\partial\rho/\partial t = 0$, the particle current density $j(x) = \rho(x)p(x)/m$ is conserved. This gives $j(x) =$ const., and we have

$$|\psi(x)|^2 = \rho(x) = \frac{mj}{p(x)}. \tag{1.12}$$

Physically speaking, the probability $\rho(x)\mathrm{d}x = j\mathrm{d}t$ is proportional to the time $\mathrm{d}t$ the particle needs to move across the interval $x \ldots x + \mathrm{d}x$ at the local velocity $p(x)/m$. Note that we cannot predict at which particular time the particle will cross the position x because the flow (the wave function) is stationary by assumption. We do not know the time when the particle started, and therefore, only a probabilistic prediction may be given.

Finally, we note from (1.12) that the WKB wave function diverges at a 'classical turning point' where the velocity vanishes. This divergence is clearly visible in figs.1.1, but it is *unphysical* (it is not reproduced by the exact solution of the SCHRÖDINGER equation).

Forbidden region

Turn now to region II in fig.1.1 that is classically forbidden because the potential is larger than the energy. The momentum

$$p(x) = \sqrt{2m(E - V(x))} = \mathrm{i}\sqrt{2m(V(x) - E)}$$

is then purely imaginary, and the wave function (1.11) shows a sort of exponential growth or decay. The local decay constant is approximately equal to $\pm|p(x)|$. The wave function shown in the figure decreases exponentially when the position x moves into the forbidden region. Whether this is physically acceptable depends on the overall behaviour of the potential.

Tunnelling through a barrier

The situation shown in fig.1.1 would be false if there were an additional potential well to the left, as shown in fig.1.2. Indeed, in this case, the particle is predominantly localised in the potential well, and (at least if the barrier is quite thick) the wave function must decrease when the position x moves towards the right into the forbidden region. On the other hand, once the barrier has been crossed, the waves 'leaks' out of the exponentially small tail towards the right. A wave propagating to the right in region I is therefore physically reasonable. This process is the 'tunnel effect', and we shall derive a simple formula for the tunnelling rate below.

Reflection from a barrier

Figure 1.3 shows the case that the forbidden region II extends up to $x = -\infty$. The exponential decay towards the left (or increase towards the right) is

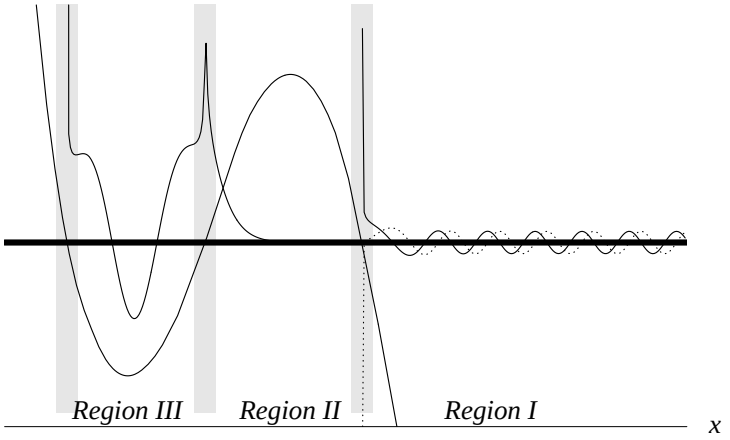

Figure 1.2: Wave function leaking out of a potential well (region III) through a barrier (II) into an allowed region (I). The waves are not matched at the transition points. The wave in region I is not drawn to scale.

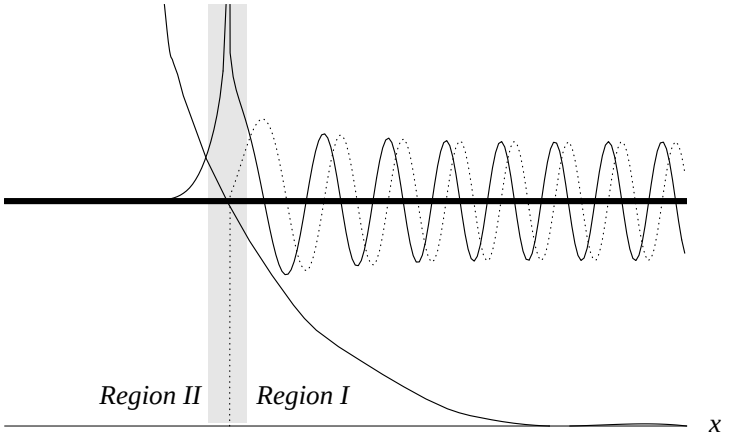

Figure 1.3: Reflection from a potential barrier. The waves are not correctly matched across the turning point, and the incident wave is missing in region I.

then physically reasonable because otherwise the total probability of being in the forbidden region would be infinite. But now, the wave function in region I is not correct: classically, one would expect that there is also a flow of particles incident from the right and being reflected from the potential barrier. The wave function must therefore contain also a term proportional to $\exp\left(-\mathrm{i}\int^x p(x')\mathrm{d}x'/\hbar\right)$, describing a wave moving towards the left. We discuss below how in this case of barrier reflection the WKB solutions are matched across the turning point.

Open questions

The discussion presented so far leads us naturally to a number of questions. They are going to be analyzed in the following sections of this chapter.

- What is a precise criterion for the validity of the WKB approximation?
- How are the WKB wave functions to be matched across the boundary between the classically allowed and forbidden regions? We anticipate that this matching depends on the global behaviour of the potential for the chosen energy (particle trapped in a well or incident from infinity, e.g.).
- The WKB wave functions should also be able to yield approximations for, e.g., the quantised energy levels in a potential well or the tunnelling rate through a barrier. We would also like to know in what regime these approximations are valid.
- How is it possible to remove the divergence $\propto 1/\sqrt{p(x)}$ of the WKB wave functions at a turning point without losing precision far away from the turning point?
- How may the above treatment be generalized to multi-component ('spinor') wave functions that are no longer scalar complex functions? And what about spatial dimensions larger than one?

1.2 Validity criteria

Naive estimate

The quantum mechanics textbooks often quote the following condition of validity of the WKB approximation: in the SCHRÖDINGER equation (**??**), we neglect

the term containing $\hbar$ compared to the others. This is reasonable if

$$\left|\frac{\hbar}{2m}\frac{\mathrm{d}^2 S}{\mathrm{d}x^2}\right| \ll \frac{1}{2m}\left(\frac{\mathrm{d}S}{\mathrm{d}x}\right)^2 \tag{1.13a}$$

where the right hand side is a particular term representing the 'large' terms in (**??**). This condition may be written in terms of the local classical momentum $p(x)$ or, equivalently, the local wavelength $\lambda(x) = \hbar/p(x)$, and we get

$$\left|\hbar\frac{\mathrm{d}p}{\mathrm{d}x}\right| \ll p^2(x) \qquad \text{or} \qquad \left|\frac{\mathrm{d}}{\mathrm{d}x}\frac{\hbar}{p(x)}\right| = \left|\frac{\mathrm{d}\lambda(x)}{\mathrm{d}x}\right| \ll 1. \tag{1.13b}$$

The WKB approximation is thus valid when *the local wavelength changes slowly*. As a rule of thumb, the gradient $\mathrm{d}/\mathrm{d}x$ in (1.13b) is of the order of $1/a$ where a is a classical length scale (that may depend on position and energy). We thus recover the intuitive idea that the DE BROGLIE wave length must be small compared to the classical length scales of the problem.

It is a simple exercise to re-write the validity condition (1.13b) in terms of the classical force acting on the particle:

$$\hbar m|F(x)| \ll p^3(x) \tag{1.13c}$$

Note that both conditions (1.13b, 1.13c) predict a breakdown of the WKB approximation at classical turning points because of the vanishing momentum $p(x)$.

On the other hand, if the wave length is spatially constant, the WKB approximation is valid (it is even exact).

More careful estimate

Recall that the WKB approximation is based on the expansion (1.6) of the action function. This expansion is accurate if higher-order terms become successively smaller in the limit of small $\hbar$. We thus obtain the condition

$$\ldots \ll \hbar^2|S_2| \ll \hbar|S_1| \ll |S_0| \tag{1.14}$$

where we have also included the second order term S_2. This term may be explicitly calculated from the SCHRÖDINGER equation, with the result (primes denotes differentiation with respect to x and S is now a complex quantity that also contains the amplitude called A before):

$$\frac{\mathrm{d}S_2}{\mathrm{d}x} = \frac{1}{2S_0'}\left(\mathrm{i}S_1'' - (S_1')^2\right) \tag{1.15}$$

This expression allows to calculate condition (1.14) for a given problem. One has to be careful with the arbitrary constants that appear in the S_n. In practice, it seems a good choice to fix a reference point x_r and to evaluate condition (1.14) for the differences $\hbar^{n-1}\left[S_n(x) - S_n(x_r)\right]$.

There is an *additional condition* that is due to the fact that the action appears in the exponent of the wave function. We have to impose that the term $\hbar S_2$ is *small compared to unity* to assure that we make only a small error in the wave function:

$$\hbar|S_2| \ll 1 \tag{1.16}$$

If this is case, we may expand

$$\exp\left[\frac{\mathrm{i}}{\hbar}\left(S_0 + \hbar S_1 + \hbar^2 S_2\right)\right] \approx \psi_{\mathrm{WKB}}(x)\left[1 + \mathrm{i}\hbar S_2(x)\right]$$

and get a correction that is small relative to the WKB wave function. If $\hbar S_2 = 0.01$, say, then the WKB wave function is accurate to one percent. Of course, condition (1.16) has also to be calculated explicitly for a given problem.

Spatially constant wave length. This an example where it is easy to obtain the actions S_n explicitly. The momentum p is constant, and choosing $x_r = 0$ as reference point, we get

$$S_0(x) = px \tag{1.17}$$

$$S_1(x) - S_1(0) = \frac{\mathrm{i}}{2}\log\frac{p(x)}{p(0)} = 0 \tag{1.18}$$

$$S_2(x) - S_2(0) = 0 \tag{1.19}$$

Both inequalities in condition (1.14) are therefore fulfilled. Furthermore, since S_2 is constant, one is free to choose $S_2 = 0$, and thus satisfy condition (1.16).

More examples are given in problem **??**. We finally note that a good check for the WKB approximation is the comparison with exactly solvable potentials. This will also be done both in the lecture and in the problems.

1.3 Matching rule at a turning point

Langer has found the following 'connection formula' for the WKB waves at a single turning point:

$$\frac{2C}{\sqrt{p(x)}}\sin\left(\frac{\pi}{4} + \frac{1}{\hbar}\int_x^{x_0} p(x')\mathrm{d}x'\right) \quad \longleftarrow$$

allowed region (I) $x < x_0$

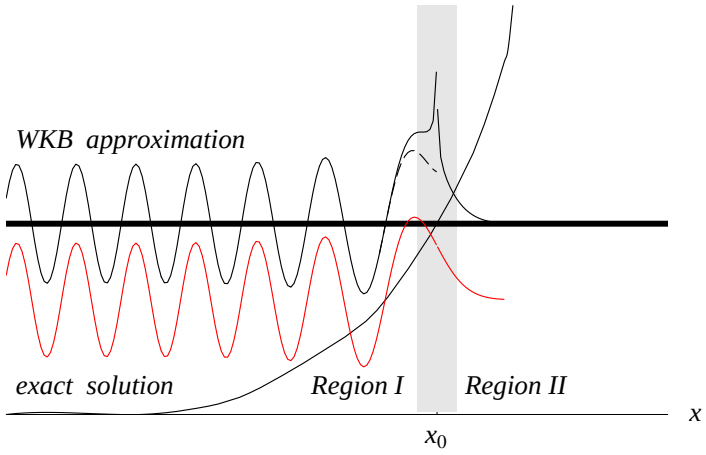

Figure 1.4: WKB wavefunction that is correctly matched at a turning point x_0. The red curve gives the (numerically computed) exact solution to the Schrödinger equation. It is shifted down because otherwise it would be indistinguishable from the WKB solution almost everywhere. The dashed curve continues the sine function in (1.20) without the $1/\sqrt{p(x)}$ divergence.

$$\longleftarrow \quad \frac{C}{\sqrt{|p(x)|}} \exp\left(-\frac{1}{\hbar}\int_{x_0}^{x} |p(x')|\mathrm{d}x'\right) \tag{1.20}$$

forbidden region (II) $x > x_0$

The arrow indicates that we got this formula by imposing a boundary condition in the forbidden region (the wave function must decrease).

The WKB wave function that results from the connection formula (1.20) is plotted in fig.1.4 and compared to the exact solution of the SCHRÖDINGER equation that was computed numerically.

Comments

- If the allowed region is located to the right of the turning point (the potential has a negative slope), the connection formula becomes

$$\frac{C}{\sqrt{|p(x)|}} \exp\left(-\frac{1}{\hbar}\int_{x}^{x_0} |p(x')|\mathrm{d}x'\right) \quad \longrightarrow$$

forbidden region (II) $x < x_0$

$$\longrightarrow \quad \frac{2C}{\sqrt{p(x)}} \sin\left(\frac{\pi}{4} + \frac{1}{\hbar}\int_{x_0}^{x} p(x')\mathrm{d}x'\right) \tag{1.21}$$

allowed region (I) $x > x_0$

Short cut: simply write the integral in such a form that their values increase when x moves away from the turning point.

- We observe in fig.1.4 that the sinusoidal oscillations in the allowed region are positioned in such a way that the inflexion point of the sine occurs at the turning point $x = x_0$ (although the amplitude of the WKB wave function still diverges). This is shown by the dashed curve in fig.1.4 where the sine function is plotted without the diverging prefactor $p(x)^{-1/2}$.

- There is a phase jump of $\pi + \pi/2 \equiv -\pi/2$ between the incident and reflected wave. It is interesting that this phase jump is intermediate between the reflection at a 'fixed' end (phase shift π) and at a 'loose' end (zero phase shift) of a string.

- The reflection probability is unity. More precisely, the reflection coefficient R is defined by the following form of the wave function in the allowed region:

$$\psi(x) = C\,[\psi_{\rm inc}(x) + R\,\psi_{\rm refl}(x)] \tag{1.22}$$

If we choose incident and reflected waves in the WKB form (1.11),

$$\psi_{\rm inc,\,refl}(x) = \frac{1}{\sqrt{p(x)}} \exp\left(\pm\frac{\rm i}{\hbar}\int_{x_0}^{x} p(x'){\rm d}x'\right)$$

we get from (1.20) a reflection coefficient

$$R = -{\rm i}$$

and hence a reflection probability $|R|^2 = 1$. On the other hand, there is zero transmission into the forbidden region. Both properties are related to the fact that the wave function is real over the entire x-axis. (Argue that this is a consequence of current conservation.)

- The connection formula (1.20) is *unidirectional* in the sense that we have started from an asymptotic condition in the forbidden region (exponential decay of the wave function). The other direction of the connection formulas is needed when a tunnelling problem is studied: one then imposes that in the allowed region, there is only an outgoing and no incoming wave. This case gives rise to both exponentially decaying and increasing solutions in the forbidden region. We study it in more detail in the following subsection. There has been a long discussion about the directionality of the connection formula; see Berry & Mount (1972) for a review of this point.

- We can derive a criterion for the validity of the above approach. Start with linearising the potential in an interval $x_0 - a \ldots x_0 + a$ whose length $2a$ must be at least a few $w = (\hbar^2/2mF)^{1/3}$. This characteristic length emerges from dimensional analysis of the Schrödinger equation in the linear potential: it gives the physical scale of the exact solutions which are provided by AIRY functions. The condition $a \gg w$ is needed because otherwise we cannot use the asymptotic expansions of the AIRY function towards the ends of the interval. This means [1]

$$a^3 \gg w^3 = \frac{\hbar^2}{2mF} \tag{1.23}$$

  This condition is of course valid if '$\hbar$ is sufficiently small'. On the other hand, it becomes violated if the classical length scale a gets too small. This length may be, for example, the distance to another turning point. If this second point comes closer than a few w's, it is in general no longer possible to treat them separately. In this case, one has to solve exactly a problem with two turning points and match the solution to the WKB wave functions that are valid at a larger distance.

1.4 Bohr-Sommerfeld quantisation

As an important application of LANGER's connection formula, we discuss here the quantum-mechanical tunnelling through a potential barrier and the semi-classical quantisation rule in an isolated potential well.

1.4.1 WKB quantisation rules

The quantisation of energy in a potential well is a second important application of LANGER's connection formula. In fig.1.5, the results that may be obtained for a generic potential are sketched. We suppose that the 'walls' of the well are impenetrable and neglect tunnelling. The physically acceptable wave function must therefore decay exponentially in the forbidden regions $x < x_1$, $x > x_2$ (where $x_{1,2}$ denote again the turning points). If the turning points are sufficiently far apart, we may use the connection formula twice to find the wave function in the allowed region $x_1 < x < x_2$. The key point is that for a generic

[1] It is interesting that we can get (1.23) from the previously derived condition (1.13b) by estimating $p \simeq \hbar/a$. This is the momentum of a particle in the ground state of a box with length a.

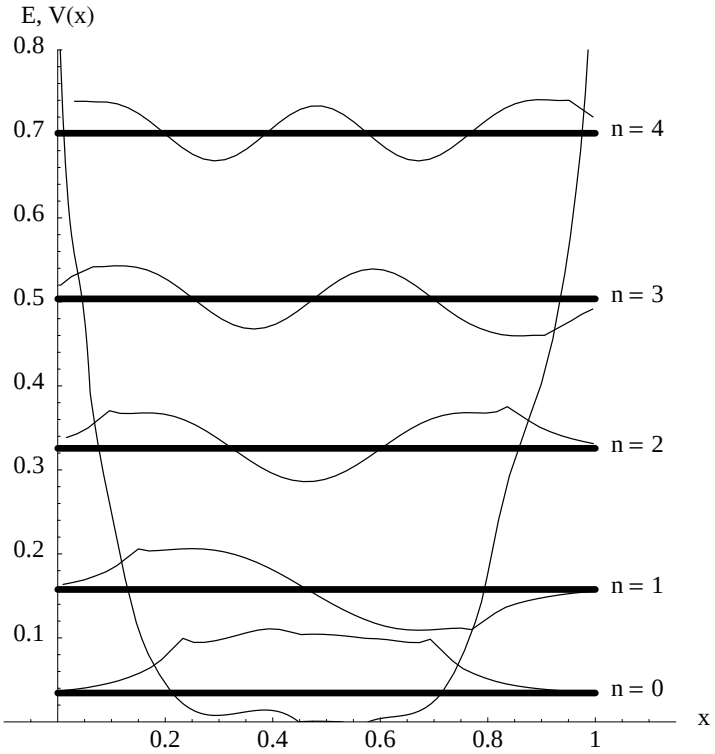

Figure 1.5: Potential well with quantised states, obtained with the semiclassical approximation.

choice of energy, we get two expressions for the wave function that do not match. To be explicit, we get from (1.21) the wave function for $x > x_1$:

$$\psi_1(x) = \frac{C}{\sqrt{p(x)}} \sin\left(\frac{\pi}{4} + \frac{1}{\hbar}\int_{x_1}^{x} p(x')\mathrm{d}x'\right), \tag{1.24}$$

while the connection formula (1.20) at the turning point x_2 gives

$$\psi_2(x) = \frac{C'}{\sqrt{p(x)}} \sin\left(\frac{\pi}{4} + \frac{1}{\hbar}\int_{x}^{x_2} p(x')\mathrm{d}x'\right). \tag{1.25}$$

To compare these two functions, we write

$$\begin{aligned}\int_x^{x_2} p(x')\mathrm{d}x' &= \int_{x_1}^{x_2} p(x')\mathrm{d}x' - \int_{x_1}^{x} p(x')\mathrm{d}x' \\ &= S(x_1, x_2) - \int_{x_1}^{x} p(x')\mathrm{d}x'\end{aligned}$$

where $S(x_1, x_2)$ is the classical action integral for half an oscillation period in the well:

$$S(x_1, x_2) = \int_{x_1}^{x_2} \sqrt{2m\left(E - V(x)\right)}\,\mathrm{d}x. \tag{1.26}$$

We thus get

$$\psi_2(x) = \frac{C'}{\sqrt{p(x)}} \sin\left(\frac{S(x_1,x_2)}{\hbar} + \frac{\pi}{2} - \frac{\pi}{4} - \frac{1}{\hbar}\int_{x_1}^{x} p(x')\mathrm{d}x'\right)$$

This function is identical to (1.24) when the first two terms in the argument of the sine are an integer multiple of π. We may then choose the constant C' equal to C up to a sign. This is the WKB quantisation rule: *the classical action must be a half-integer multiple of the Planck constant:*[2]

$$\begin{aligned} S(x_1,x_2) &= \left(n+\tfrac{1}{2}\right)\pi\hbar, \qquad n = 0,\, 1,\, 2,\, \ldots \\ C' &= (-1)^n C, \end{aligned} \tag{1.27}$$

Observe that depending on the parity of the quantum number, the eigenfunctions decay with the same sign or with different signs in the forbidden regions (see fig.1.5). This is reminiscent of the well-defined parity of the eigenfunctions in an even potential well.

The accuracy of the semiclassical approximation can be checked from the validity criteria given before: one has to compare the distance between the turning points to the length scales $w_{1,2}$ that appear in the WKB matching procedure at the turning points. The ground state wave function $n = 0$ shown in fig.1.5, e.g., is certainly inaccurate because it shows inflexion points in a region where both the potential and the wave function do not vanish.

It is not too easy to determine eigenvalues numerically, and for this reason the semiclassical formula (1.27) is useful, too. Typically one uses the 'shooting method': first, a trial value for E close to the semiclassical eigenvalue is chosen; then the Schrödinger equation is solved starting from a point deep in the forbidden region $x < x_1$. This solution typically diverges exponentially in the forbidden region $x > x_2$. Then the energy is changed until the sign of this divergence changes. One can then use successive bisections to find the energy where the wave function becomes smaller than a preset accuracy. It also helps to study the semiclassical wave functions when choosing the initial and final points in the forbidden regions.

Examples

For a *harmonic* potential, the WKB quantisation procedure reproduces the exact eigenvalues. Although this happens by accident (check it from the WKB validity

[2]The integer n must be non-negative because the action integral (1.26) is positive.

criteria), it is nevertheless a simple nontrivial example. The action integral is

$$\sqrt{2m}\int_{x_1}^{x_2}\sqrt{E-\tfrac{m}{2}\omega^2x^2}\,\mathrm{d}x = m\omega\frac{\pi x_2^2}{2} = \frac{\pi E}{\omega}$$

and the quantisation rule (1.27) gives $E = E_n = \left(n+\frac{1}{2}\right)\hbar\omega$.

For a *linear* potential well that is closed by an infinite potential barrier (Wallis & al., 1992), the WKB quantisation rule applies with a slight modification: there is no phase jump $\pi/4$ at the infinite barrier. We thus get

$$\begin{aligned}\sqrt{2m}\int_0^{x_2}\sqrt{E-Fx}\,\mathrm{d}x = \sqrt{2mF}\frac{2(E/F)^{3/2}}{3} &\stackrel{!}{=} \left(n+\tfrac{1}{4}\right)\pi\hbar \\ \Longrightarrow \quad E_n = \left[\frac{3\pi}{2}\left(n+\tfrac{1}{4}\right)\right]^{2/3} Fw &\end{aligned} \tag{1.28}$$

where w is the length scale for the linear potential introduced in (**??**). Note the different power law $E \propto n^{2/3}$ as compared to the harmonic potential.

Since we know the exact wave function for the linear potential, we can evaluate the accuracy of the WKB approximation. The exact wave function is given by a displaced AIRY function $\mathrm{Ai}((x-x_2)/w)$, where $x_2 = E/F$ is the right turning point. The boundary condition at $x_1 = 0$ imposes the quantisation of energy:

$$\mathrm{Ai}(-E/Fw) = 0$$

The energy eigenvalues are thus proportional to the zeros of the AIRY function, with the quantity Fw giving the energy scale. Figure 1.6 compares this result with the semiclassical prediction. One sees that for $n \geq 10$ the agreement is already quite good.

Other examples are the Eckart or Morse wells

$$\begin{aligned} V(x) &= \frac{V_0}{\cosh^2(\kappa x)}, \\ V(x) &= V_0\left(\mathrm{e}^{-\kappa x}-1\right)^2 \end{aligned}$$

where exact eigenfunctions and eigenvalues may be obtained. These potentials are studied as problems.

1.4.2 Barrier tunnelling

(*Material not covered in WS 2012/13.*)

Consider a wave that is scattered by a potential barrier, as shown in fig.1.7. We shall suppose that the particle is incident from $x \to -\infty$ where the potential is small,

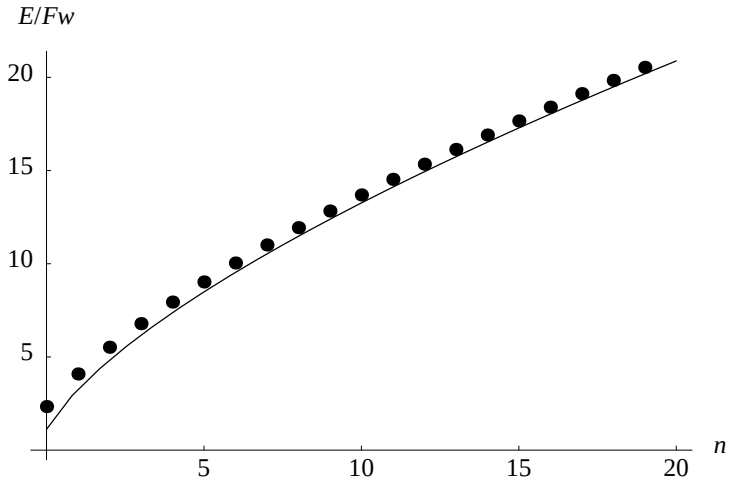

Figure 1.6: Quantised energy values in a linear potential well. Dots: exact zeroes of the AIRY function; line: semiclassical prediction (1.28).

and that its energy is below the barrier top. We have two turning points $x_{1,2}$ and the following asymptotic behaviours:

$$x \to -\infty: \qquad \psi(x) = \text{incident wave} + R\,\text{reflected wave}$$
$$x \to +\infty: \qquad \psi(x) = T\,\text{transmitted wave}$$

Note that to the right of the barrier, there is only a single transmitted and no incident wave. As a consequence, the wave function will be complex. We shall construct a suitable superposition of real wave functions, and for this purpose, we need a second wave function that solves the turning point problem.

Matching with an exponentially growing wave at a turning point. In the previous section, we constructed a physically acceptable wave function at a reflecting

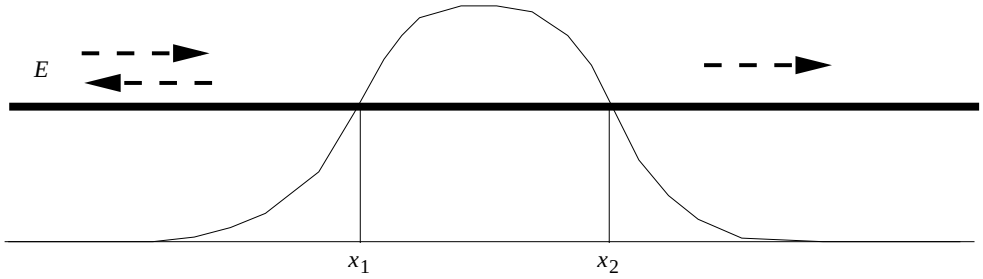

Figure 1.7: Reflection and transmission of a wave from a potential barrier.

turning point. We consider here the opposite case, namely a wave function that diverges in the forbidden region. This divergence is not a real problem because for the barrier shown in fig.1.7, the forbidden region has a finite extension.

The calculation is quite parallel to the one in the previous section. We choose again the dimensionless variable ξ with $\xi > 0$ being the forbidden region. The AIRY equation (**??**) has the second solution $\mathrm{Bi}(\xi)$ that is sketched in fig.1.8. It shows an exponen-

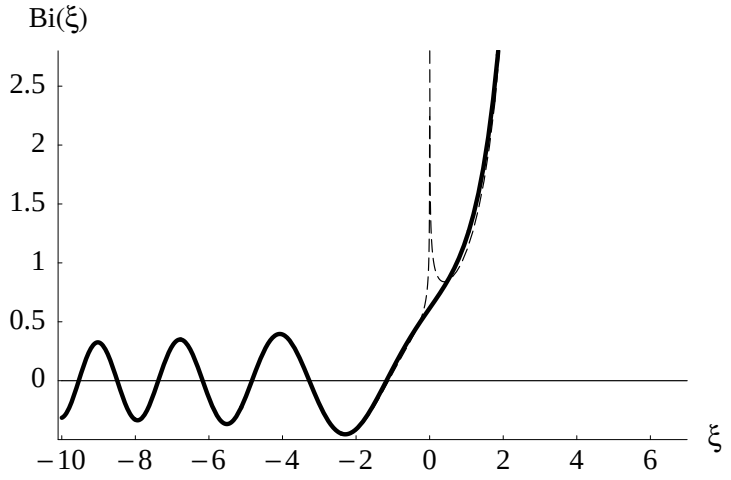

Figure 1.8: The AIRY function $\mathrm{Bi}(x)$ (solid curve) and its asymptotic forms (dashed curves).

tial growth in the forbidden region. The asymptotic behaviours are (see problem **??**)

$$\xi \ll -1 : \mathrm{Bi}(\xi) \approx \frac{1}{\sqrt{\pi}(-\xi)^{1/4}} \cos\left[\frac{2}{3}(-\xi)^{3/2} + \frac{\pi}{4}\right] \tag{1.29a}$$

$$\xi \gg 1 : \mathrm{Bi}(\xi) \approx \frac{1}{\sqrt{\pi}\xi^{1/4}} \exp\left[\frac{2}{3}\xi^{3/2}\right] \tag{1.29b}$$

Note the factor of 2 that is missing in (1.29b) and the cos instead of the sin in (1.29a). When we compare these formula to the WKB wave functions in the vicinity of the turning point, we arrive at the following connection formula

$$\begin{aligned} &\frac{D}{\sqrt{p(x)}} \cos\left(\frac{\pi}{4} + \frac{1}{\hbar}\int_x^{x_0} p(x')\mathrm{d}x'\right) \longrightarrow \\ &\qquad \text{allowed region (I) } x < x_0 \\ &\longrightarrow \frac{D}{\sqrt{|p(x)|}} \exp\left(\frac{1}{\hbar}\int_{x_0}^{x} |p(x')|\mathrm{d}x'\right) \\ &\qquad \text{forbidden region (II) } x > x_0 \end{aligned} \tag{1.30}$$

Berry & Mount (1972) quote the warning of Fröman & Fröman (1965) that this connection formula has to be taken with much care. Indeed, eq.(1.30) may only be understood

as a relation between the asymptotic behaviour of this (unphysical) wave function. In numerical work, it is impossible to be sure that the decaying exponential has a nonzero coefficient – this does not change the numerical results just because the coefficient is multiplied by a small number. But a nonzero coefficient inevitably gives an admixture of a sine function in the allowed region and changes the phase of the standing wave. The derivation used here shows that (1.30) simply gives the asymptotic form of the other linearly independent solution to the SCHRÖDINGER equation.

The turning point x_2. The status of the connection formula (1.30) thus clarified, we can write it down for the turning point x_2 in fig.1.7. In this case, the forbidden region is located to the left of x_2, and the connection formula becomes

$$\begin{aligned} &\frac{D}{\sqrt{|p(x)|}} \exp\left(\frac{1}{\hbar}\int_x^{x_0} |p(x')|\mathrm{d}x'\right) \quad \longleftarrow \\ &\qquad \text{forbidden region (II) } x < x_0 \\ &\longleftarrow \quad \frac{D}{\sqrt{p(x)}} \cos\left(\frac{\pi}{4} + \frac{1}{\hbar}\int_{x_0}^{x} p(x')\mathrm{d}x'\right) \\ &\qquad \text{allowed region (I) } x > x_0 \end{aligned} \tag{1.31}$$

If we want to get a transmitted wave propagating to the right

$$x > x_2 : \quad \psi(x) = \frac{N}{\sqrt{p(x)}} \exp\left(\frac{\mathrm{i}}{\hbar}\int_{x_2}^{x} p(x')\mathrm{d}x' + \frac{\mathrm{i}\pi}{4}\right),$$

we thus have to superpose the wave functions (1.21, 1.31) with the coefficients

$$2C = \mathrm{i}N, \qquad D = N$$

where N is a global normalisation constant. 'Under the potential barrier' (in the forbidden region), the wave function is a superposition of exponentially growing and decreasing waves with weights given by C, D. We now match this superposition to incident and reflected waves at the first turning point x_1. To simplify the comparison, we write

$$\begin{aligned} \int_x^{x_2} |p(x')|\mathrm{d}x' &= \int_{x_1}^{x_2} |p(x')|\mathrm{d}x' - \int_{x_1}^{x} |p(x')|\mathrm{d}x' \\ &= \hbar W - \int_{x_1}^{x} |p(x')|\mathrm{d}x' \end{aligned}$$

where W is a positive number that depends on the energy and the behaviour of the potential in the forbidden region

$$W = \frac{\sqrt{2m}}{\hbar}\int_{x_1}^{x_2} \sqrt{V(x') - E}\,\mathrm{d}x' \tag{1.32}$$

The turning point x_1. The wave function that arrives from the right at the turning point x_1 is thus of the form

$$x > x_1: \quad \psi(x) = \frac{N}{\sqrt{|p(x)|}} \left[\mathrm{e}^{W} \exp\left(-\frac{1}{\hbar} \int_{x_1}^{x} |p(x')| \mathrm{d}x' \right) + \right. \\ \left. + \frac{\mathrm{i}}{2} \mathrm{e}^{-W} \exp\left(\frac{1}{\hbar} \int_{x_1}^{x} |p(x')| \mathrm{d}x' \right) \right] \tag{1.33}$$

The first term decreases when x moves into the forbidden region and therefore connects to the regular solution of formula (1.20). For the second, increasing term we need again the connection formula (1.30) for the 'unphysical' solution. We finally get, in the allowed region $x < x_1$, the following superposition of incident and reflected waves

$$x < x_1: \quad \psi(x) = \frac{N}{\sqrt{p(x)}} \left[\alpha_{\mathrm{inc}} \exp\left(\frac{\mathrm{i}}{\hbar} \int_{x_1}^{x} p(x') \mathrm{d}x' \right) + \right. \\ \left. + \alpha_{\mathrm{refl}} \exp\left(-\frac{\mathrm{i}}{\hbar} \int_{x_1}^{x} p(x') \mathrm{d}x' \right) \right]$$

where the coefficients are given by

$$\alpha_{\mathrm{inc}} = \mathrm{e}^{W + \mathrm{i}\pi/4} \left(1 + \tfrac{1}{4} \mathrm{e}^{-2W} \right), \tag{1.34}$$

$$\alpha_{\mathrm{refl}} = \mathrm{e}^{W - \mathrm{i}\pi/4} \left(1 - \tfrac{1}{4} \mathrm{e}^{-2W} \right). \tag{1.35}$$

Using the fact that the WKB wave functions have unit flux, we thus get the following reflection and transmission coefficients:

$$R = -\mathrm{i} \frac{1 - \frac{1}{4}\mathrm{e}^{-2W}}{1 + \frac{1}{4}\mathrm{e}^{-2W}}, \qquad |R|^2 \approx 1 - \mathrm{e}^{-2W} \tag{1.36a}$$

$$T = \frac{\mathrm{e}^{-W}}{1 + \frac{1}{4}\mathrm{e}^{-2W}}, \qquad |T|^2 \approx \mathrm{e}^{-2W} \tag{1.36b}$$

where the approximations are valid when $W \gg 1$ (semiclassical regime: 'action integral' (1.32) large compared to $\hbar$). We observe that in this regime, the transmission through the barrier is extremely small: the current is transported to the second turning point x_2 only via the 'tail' of the exponentially decaying wave that enters the forbidden region at x_1.

Comments. One may verify from (1.36) that current conservation, $|R|^2 + |T|^2 = 1$, is also valid if W is not large. In this limit, however, the turning points $x_{1,2}$ approach each other too closely to allow for a separate application of the single turning point connection formula, and the results (1.36) cease to be valid. In problem **??**, you are invited to derive an approximation that covers this regime. One result of this approximation is that when the incident energy coincides with the barrier top, both reflection and transmission probabilities $|R|^2$ and $|T|^2$ are equal to $\frac{1}{2}$. For energies below the barrier, the transmission decreases rapidly to exponentially small values. But even when

the energy is larger than the barrier top, there is a nonzero probability of reflection. It becomes very small, too, when the energy is much larger than the barrier top.

We can get a simple estimate for the width in energy of the transition zone where the transmission goes over from close to zero to close to unity. Close to the barrier top, we approximate the potential by an inverted parabola with second derivative $V'' = -m\omega^2$. For an energy ΔE below the barrier top, two turning points exists and are spaced

$$a = \sqrt{\frac{8\Delta E}{m\omega^2}}$$

apart. In the estimate (1.23) for the validity of the single turning point connection formula, we have to require $a \gg w$ where w depends on the potential slope at the turning points. Using the definition (**??**) of the width w, we find that our result is valid provided $\Delta E \gg \hbar\omega/8$, i.e., the energy is sufficiently below the barrier top. This condition implies in turn that the transmission through the barrier is very small since we have (using again a parabolic shape for the barrier top) $W \approx \pi\Delta E/\hbar\omega \gg \pi/8 \approx 0.393$.

> **Remark.** LANGER was not the first to use the patching procedure with the AIRY function at a turning point. This method was already employed by JEFFREYS (1923) and KRAMERS (1926). The other two people in what is sometimes called the JWKB approximation are WENZEL and BRILLOUIN.

1.5 Uniform asymptotic approximations

1.5.1 The basic idea

LANGER's connection formula tells us how to glue the WKB wave functions together on both sides of a turning point. But we still have a wave function that is made up of two or three different expressions, depending on whether the AIRY function is used close to the turning point or not. It would be great if we had a single formula that is valid throughout the transition region. Such a kind of formula exists, and in fact LANGER already wrote it in his papers.

Langer (1937) was able to derive a *uniform asymptotic* approximation to the wave function at a single turning point. His results were subsequently generalised, and are based on the following idea (Berry & Mount, 1972). We want an approximate solution of the Schrödinger equation[3]

$$-\frac{\mathrm{d}^2\psi}{\mathrm{d}x^2} + W(x)\psi = 0, \tag{1.37a}$$

[3]To simplify the notation, we write the potential in the form $W(x) = (2m/\hbar^2)\,[V(x) - E]$.

and we know the exact solution $\phi(y)$ to a 'similar', but simpler potential $U(y)$,

$$-\frac{\mathrm{d}^2\phi}{\mathrm{d}y^2} + U(y)\phi = 0. \tag{1.37b}$$

This equation is called the 'comparison equation'. We conjecture that the wave function $\phi(y)$ will be similar to $\psi(x)$ and may be obtained by 'streching or contracting it a little and changing the amplitude a little' (Berry & Mount, 1972, p.343). We thus make the *ansatz*

$$\psi(x) = f(x)\phi(y(x)) \tag{1.38}$$

where $f(x)$ and $y(x)$ are functions to be determined. Insert this into the SCHRÖDINGER equation (1.37a) and find, using (1.37b):

$$-\frac{\mathrm{d}^2 f}{\mathrm{d}x^2}\phi - \frac{\mathrm{d}\phi}{\mathrm{d}y}\left(2\frac{\mathrm{d}f}{\mathrm{d}x}\frac{\mathrm{d}y}{\mathrm{d}x} + f\frac{\mathrm{d}^2 y}{\mathrm{d}x^2}\right) - f\left(\frac{\mathrm{d}y}{\mathrm{d}x}\right)^2 U\,\phi + f\,W\,\phi = 0. \tag{1.39}$$

We can get rid of the first derivative $\mathrm{d}\phi/\mathrm{d}y$ by choosing

$$f = \left(\frac{\mathrm{d}y}{\mathrm{d}x}\right)^{-1/2} \tag{1.40}$$

Then we may divide by $f\,\phi$ and find an equation for the 'coordinate mapping' $y(x)$:

$$-\left(\frac{\mathrm{d}y}{\mathrm{d}x}\right)^{1/2}\frac{\mathrm{d}^2}{\mathrm{d}x^2}\left(\frac{\mathrm{d}y}{\mathrm{d}x}\right)^{-1/2} - \left(\frac{\mathrm{d}y}{\mathrm{d}x}\right)^2 U(y(x)) + W(x) = 0 \tag{1.41}$$

We now make an approximation that is motivated by our idea that the coordinates x and y differ only by small strechtings. We can then expect that the second derivative in (1.41) to be 'small', and may neglect it.[4] We then get the first-order differential equation

$$\frac{\mathrm{d}y}{\mathrm{d}x} = \pm\left(\frac{W(x)}{U(y(x))}\right)^{1/2} \tag{1.42}$$

With the initial condition $y(x_0) = y_0$, we find the following implicit solution

$$\int_{x_0}^{x}\sqrt{W(x')}\,\mathrm{d}x' = \pm\int_{y_0}^{y}\sqrt{U(y')}\,\mathrm{d}y' \tag{1.43a}$$

$$\int_{x}^{x_0}\sqrt{-W(x')}\,\mathrm{d}x' = \pm\int_{y}^{y_0}\sqrt{-U(y')}\,\mathrm{d}y' \tag{1.43b}$$

[4]This procedure is similar to what we did at the start to get the WKB approximation.

where the choice depends on the sign of $W(x)$, i.e., whether x is in an allowed ($W(x) < 0$) or forbidden ($W(x) > 0$) region (see footnote 3 on p. 23).

Once we have computed $y(x)$ by inverting these equations, we have the following approximation for the wave function

$$\psi(x) \approx \left[\frac{U(y(x))}{W(x)}\right]^{1/4} \phi(y(x)) \tag{1.44}$$

We shall see that this solution is valid for the whole range of x, even close to turning points.

This method works only when the coordinate mapping $x \mapsto y(x)$ is bijective, i.e., when the derivative $\mathrm{d}y/\mathrm{d}x$ is nowhere zero nor infinite. Looking at (1.42), we observe that this implies that the zeros of the potentials $W(x)$ and $U(y)$ are mapped onto each other. In particular, both potentials must have the same number of turning points. 'We thus have what is potentially a very powerful principle: in the semiclassical limit all problems are equivalent which have the same *classical turning-point structure*' (Berry & Mount, 1972, p.344).

1.5.2 Examples

Recover the standard WKB waves. The first example is a *classically allowed region without turning points*. The function $W(x) = -p^2(x)/\hbar^2$ then vanishes nowhere, and we may take $U(y) \equiv -1$. The comparison equation reads

$$\frac{\mathrm{d}^2\phi}{\mathrm{d}y^2} + \phi = 0$$

and its solutions are plane waves $\phi = \exp(\pm \mathrm{i}y)$. The coordinate mapping is obtained from the solution of

$$\frac{\mathrm{d}y}{\mathrm{d}x} = \pm\frac{p(x)}{\hbar}. \tag{1.45}$$

The amplitude function (1.40) is thus equal to $f(x) = (\hbar/p(x))^{1/2}$, and we get the propagating WKB waves

$$\psi(x) \approx \frac{C}{\sqrt{p(x)}} \exp\left(\pm\frac{\mathrm{i}}{\hbar}\int_{x_0}^{x} p(x')\,\mathrm{d}x'\right).$$

These expressions are no longer valid at turning points because the mapping $x \mapsto y$ then becomes singular [see (1.45)]. Similarly, we can derive the WKB solutions in classically forbidden regions by choosing $U(y) \equiv 1$.

A single turning point. If the potential $W(x) = -p^2(x)/\hbar^2$ has a simple turning point at, say, x_0, we are advised to take a comparison potential with a simple zero, say, $U(y) = y$. This gives the AIRY equation

$$-\frac{\mathrm{d}^2\phi}{\mathrm{d}y^2} + y\phi = 0$$

with the general solution $\phi(y) = \alpha\mathrm{Ai}(y) + \beta\mathrm{Bi}(y)$. To compute the coordinate mapping, we observe from (1.42) that the classically allowed region $W(x) < 0$ must be mapped onto $y < 0$, and vice versa. This fixes the sign of the derivative $\mathrm{d}y/\mathrm{d}x$. Suppose for definiteness that the allowed region is $x < x_0$. We thus get from the implicit coordinate mapping (1.43)

$$\frac{2}{3}(-y)^{3/2} = \frac{1}{\hbar}\int_x^{x_0} p(x')\,\mathrm{d}x',\ x \in \text{allowed},\ y < 0 \tag{1.46a}$$

$$\frac{2}{3}y^{3/2} = \frac{1}{\hbar}\int_x^{x_0} |p(x')|\,\mathrm{d}x',\ x \in \text{forbidden},\ y > 0 \tag{1.46b}$$

If the allowed and forbidden regions are located the other way round, one simply has to change the order of the integration limits. The mapping (1.46) thus makes those points x, y correspond for which the classical action integral (divided by $\hbar$) has the same value. Recalling the expansion of the action in the vicinity of the turning point, we also conclude that the mapping $x \mapsto y = (\operatorname{sign} V'(x_0))(x - x_0)/w$ is approximately linear there. This justifies *a posteriori* the neglect of the second derivative in (1.41) around the turning point (the function $\mathrm{d}y/\mathrm{d}x$ is approximately constant).

Finally, we get the following uniform approximation for the wave function for a potential with a single turning point:

$$\psi(x) = C\left(\frac{y(x)}{p^2(x)}\right)^{1/4}\Big(\alpha\mathrm{Ai}(y(x)) + \beta\mathrm{Bi}(y(x))\Big) \tag{1.47}$$

It is a simple exercise to check that far from the turning point, this expression goes over into both connection formulas (1.20, 1.30): the argument $y(x)$ is then large in magnitude, and we may use the asymptotic expansions of the AIRY functions. Because of the form (1.46) of the coordinate mapping, we then recover exponentials or trigonometric functions whose arguments are classical action integrals.

Explicit example: uniform expansion for the BESSEL functions. To illustrate the power of the uniform expansion, we shall derive a uniform expansion

of the BESSEL functions. It has been shown in problem **??** that the BESSEL function $J_n(kr)$ is the physically acceptable solution to the radial SCHRÖDINGER equation

$$-\frac{\mathrm{d}^2}{\mathrm{d}r^2}J_n - \frac{1}{r}\frac{\mathrm{d}}{\mathrm{d}r}J_n + \frac{n^2}{r^2}J_n = k^2 J_n$$

where r is the radius in (two-dimensional) polar coordinates. To simplify the following calculations, we measure r in units of $1/k$ and put $k = 1$. We get rid of the first derivative in the BESSEL equation by putting

$$J_n(r) = \frac{1}{\sqrt{r}}j(r)$$

The physical boundary condition at the origin is now that $j(r)$ is of order $r^{n+1/2}$ there. The centrifugal potential then changes to

$$\frac{n^2}{r^2} \mapsto \frac{n^2 - \frac{3}{4}}{r^2} \equiv \frac{L^2}{r^2},$$

and we find the following potential

$$W(r) = \frac{L^2}{r^2} - 1$$

This potential has a single turning point at $r_0 = L$ (note that this zero does not exist when $n = 0$, we exclude this case). We map the forbidden region $0 < r < r_0$ onto the half-axis $y > 0$ of the AIRY equation using (1.46) and get

$$\begin{aligned}\frac{2}{3}y^{3/2} &= \int_r^{r_0}\sqrt{W(r')}\,\mathrm{d}r' = \int_r^{r_0}\sqrt{L^2 - r'^2}\frac{\mathrm{d}r'}{r'} \\ &= L\log\left(\frac{L + \sqrt{L^2 - r^2}}{r}\right) - \sqrt{L^2 - r^2}\end{aligned}$$

Similarly, the allowed region $r_0 < r < \infty$ is mapped onto $y < 0$ using

$$\begin{aligned}\frac{2}{3}(-y)^{3/2} &= \int_{r_0}^{r}\sqrt{r'^2 - L^2}\frac{\mathrm{d}r'}{r'} \\ &= L\arcsin\frac{L}{r} + \sqrt{r^2 - L^2} - L\frac{\pi}{2}.\end{aligned}$$

The prefactor of the wave function is given by $(y(x)/W(x))^{1/4}$. The coordinate mapping is illustrated in Fig.1.9(left) for different values of L. Note how $y(r)$ is smooth at $r = L = r_0$.

Using the boundary condition that the BESSEL functions $J_n(kr)$ vanish at the origin (for $n \geq 1$), we finally get the following asymptotic expression

$$J_n(kr) = C\left(\frac{y(kr)}{n^2 - \frac{3}{4} - k^2r^2}\right)^{1/4}\mathrm{Ai}(y(kr)) \qquad (1.48)$$

The uniform approximation cannot determine the global prefactor C. but comparing with the standard asymptotic form of the BESSEL functions for large argument $kr \gg n$, we find $C = \sqrt{2}$. Comparing to the standard asymptotics, one also finds that the uniform expansion is valid if the effective angular momentum L is large compared to unity.

In fig.1.9(right), we compare the uniform expansion (1.48) to the exact BESSEL functions $J_n(kr)$ for several values of n. We observe that the agreement

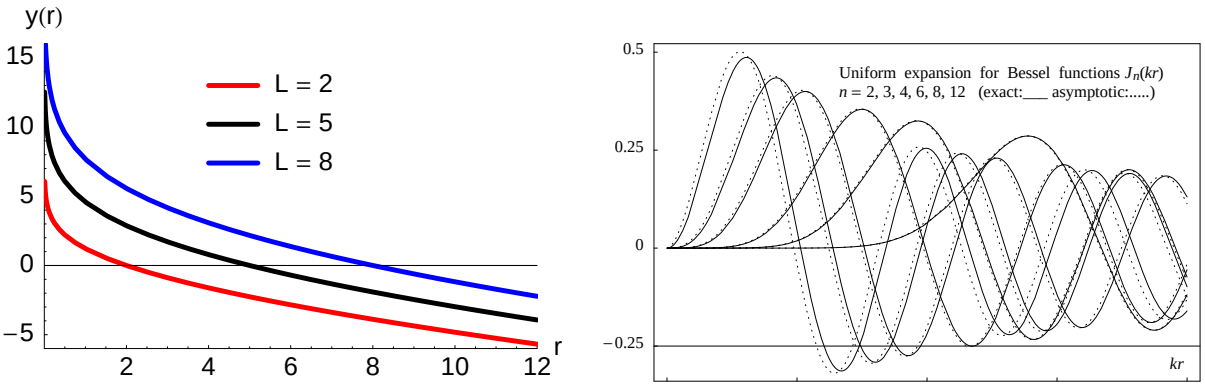

Figure 1.9: Uniform asymptotic expansion (1.48) for the BESSEL functions.

is quite good over the entire range of the argument kr and becomes much better when the order n (and hence the effective angular momentum L) increases.

1.6 Multi-state dynamics

Motivation

There are a number of fields in physics where a particle or a particle system may exist in different states. These states are, typically, subject to different potentials. An example is a molecule made of two atoms. Depending on the electronic state of the atoms, the relative motion is governed by attractive or repulsive potentials (see figure 1.11). How does the Schrödinger equation look like for such a system? It still depends on a single coordinate (the relative distance of the two atoms in the above example), but we have to use a wave function with two components, each one giving the probability amplitude to be in the state $\alpha = 1, 2$. We shall call such an object $\Psi(x)$ a 'spinor'. Similarly, the potential becomes a 2×2 matrix.

1.6.1 Light polarization and geometrical optics

Another example with a similar formal structure is electrodynamics in the limit where the wavelength is small, also known as geometrical optics. We know that the electromagnetic field is a vector field, described by the Maxwell equations

$$\begin{aligned} \nabla \times \mathbf{B} + \mathrm{i}\frac{\omega}{c^2}\varepsilon(\mathbf{x})\mathbf{E} &= 0 \\ \nabla \times \mathbf{E} - \mathrm{i}\omega\varepsilon(\mathbf{x})\mathbf{B} &= 0 \end{aligned} \tag{1.49}$$

This is written in SI units, at a fixed frequency ω and in a medium with permittivity $\varepsilon(\mathbf{r}, \omega)$ (also known as dielectric function). We assume in the following that $\varepsilon = n^2$ is real. The symmetry between $\mathbf{E}$ and $\mathbf{B}$ can be restored by rescaling the magnetic field to $c\mathbf{B} = \mathbf{H}$. We introduce the wavenumber $k = \omega/c$.

We consider the asmptotic limit of a small wavelength where $\lambda\!\!\!^{-} = 1/k \to 0$ plays the role of the Planck constant. This motivates the *Ansatz*

$$\mathbf{E}(\mathbf{x}) = \mathcal{E}(\mathbf{x})\,\mathrm{e}^{\mathrm{i}kS(\mathbf{x})}, \qquad \mathbf{H}(\mathbf{x}) = \mathcal{H}(\mathbf{x})\,\mathrm{e}^{\mathrm{i}kS(\mathbf{x})} \tag{1.50}$$

with slowly varying vector amplitudes $\mathcal{E}$ and $\mathcal{H}$. The function $S(\mathbf{x})$ is called the *eikonal*. Putting this into the Maxwell equations (1.49), we find to leading order in $\lambda\!\!\!^{-}$:

$$\nabla S \times \mathcal{H} + n^2\mathcal{E} = 0, \quad \nabla S \times \mathcal{E} - \mathcal{H} = 0 \quad \Rightarrow \quad (\nabla S)^2 = n^2 \tag{1.51}$$

which is known as the *eikonal equation*. Note the similarity to the WKB result for the action. We can make the formal analogy $n^2(\mathbf{x}) \leftrightarrow E - V(\mathbf{x})$ to the potential of classical mechanics. In the vector case we are dealing with here, we get additional information: the amplitude vectors $\mathcal{E}$ and $\mathcal{H}$ are both orthogonal to the gradient ∇S, the three forming a so-called *Dreibein*. This is sometimes called an 'solvability condition': it corresponds to constraints that are built into the partial differential equations, and that the solutions must satisfy (similar to $\nabla \cdot \mathbf{B} = 0$).

To solve the eikonal equation, one introduces the *light rays* $\mathbf{r}(s)$ as the field lines of the vector field ∇S. By definition of field lines, they solve the differential equation

$$\frac{\mathrm{d}\mathbf{r}}{\mathrm{d}s} \sim \nabla S[\mathbf{r}(s)], \qquad \frac{\mathrm{d}\mathbf{r}}{\mathrm{d}s} = \frac{\nabla S[\mathbf{r}(s)]}{n[\mathbf{r}(s)]} \tag{1.52}$$

where in the second step, we have chosen the parameter s to be the arc length of the ray: recall that the vector $\nabla S/n$ is a unit vector according to the eikonal equation (1.51). Eq.(1.52) is still not very useful because it involves the function ∇S that we do not know yet. One can eliminate the eikonal, however, by

calculating the 'acceleration' (second derivative) of the ray

$$\frac{\mathrm{d}}{\mathrm{d}s} n[\mathbf{r}(s)] \frac{\mathrm{d}\mathbf{r}}{\mathrm{d}s} = \nabla n[\mathbf{r}(s)] \tag{1.53}$$

This is the basic equation of geometrical optics. Note again the analogy to mechanics, with ∇n playing the role of the 'force'. In a homogeneous medium, the rays are therefore straight lines.

Intensity and polarization transport. Along a light ray (more precisely: a bundle of rays), one can show that the electromagnetic energy density is flowing with a current density given by the Poynting vector. By analogy to the continuity equation,

$$\nabla \cdot \mathrm{Re}\, \mathcal{E}^* \times \mathbf{H} = 0 \tag{1.54}$$

(a factor n may be missing here). For the transport of the polarization vectors, we introduce the (complex) unit vectors

$$\mathbf{e} = \frac{\mathcal{E}}{|\mathcal{E}|}, \quad \mathbf{h} = \frac{\mathcal{H}}{|\mathcal{H}|} \tag{1.55}$$

and find (see the book by Born & Wolf (1959) for details)

$$n(\mathbf{r}) \frac{\mathrm{d}\mathbf{e}}{\mathrm{d}s} = -(\mathbf{e} \cdot \nabla \log n) \nabla S \tag{1.56}$$

To interpret this equation, consider the simple case that the ray is lying in a plane spanned by the vectors ∇S (the tangent or velocity vector) and ∇n (the acceleration). If $\mathbf{e}$ is perpendicular to this plane, then from Eq.(1.56), it does not change and remains perpendicular. On the other hand, if $\mathbf{e}$ is in the ray plane, Eq.(1.56) forces it to change. Using the fact that $\mathbf{e}$ and ∇S are perpendicular [solvability condition (1.51)], we can re-write Eq.(1.56) into

$$\begin{aligned} n(\mathbf{r}) \frac{\mathrm{d}\mathbf{e}}{\mathrm{d}s} &= -(\mathbf{e} \cdot \nabla \log n) \nabla S + \underbrace{(\mathbf{e} \cdot \nabla S)}_{=0} \nabla \log n \\ &= (\nabla S \times \nabla \log n) \times \mathbf{e} \end{aligned} \tag{1.57}$$

This means that the polarization vector is rotating in the ray plane (around an axis $\nabla S \times \nabla \log n$ perpendicular to the ray plane). One ensures in this way that $\mathbf{e}$ remains perpendicular to ∇S. In differential geometry, this process is called '*parallel transport*' of the *Dreibein* (see Fig.1.10).

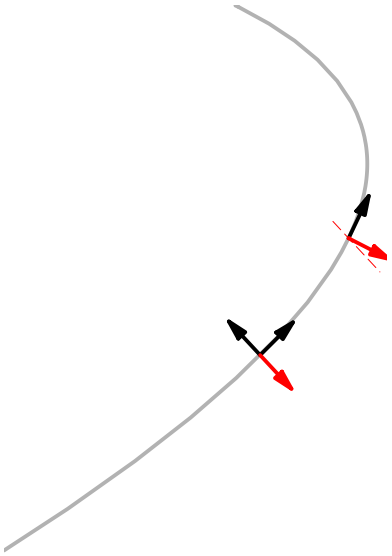

Figure 1.10: Illustration of parallel transport of polarization along a curved light ray. The black arrows illustrate the tangent vector ∇S and the index gradient ∇n ('force'). The red arrows give the electric field vector at two positions along the ray. The dashed line is parallel to the polarization vector at the upstream position.

1.6.2 Spinor wave functions

For a spinor wave function with two components, the Schrödinger equation reads

$$\mathrm{i}\hbar\frac{\partial\Psi(x,t)}{\partial t} = -\frac{\hbar^2}{2m}\frac{\partial^2\Psi(x,t)}{\partial x^2} + V(x)\Psi(x,t) \tag{1.58}$$

The potential matrix $V(x)$ is hermitian,

$$V(x) = \begin{pmatrix} V_{11}(x) & V_{12}(x) \\ V_{21}(x) & V_{22}(x) \end{pmatrix}, \quad V_{12} = V_{21}^*, \tag{1.59}$$

and its diagonal elements $V_{\alpha\alpha}(x)$ give the potentials shown in fig.1.11. The off-diagonal element $V_{12}(x)$ describes the *coupling* between the potentials. For the molecule, one might think of a laser field that excites the atoms from one to the other electronic state. If the off-diagonal elements of the potential is zero, the Schrödinger equation (1.58) decouples into two separate scalar equations for the spinor components $\psi_\alpha(x)$. We can then apply the semiclassical techniques described above.

We get a qualitatively different behaviour when the coupling is nonzero. For example, if the particle is initially in the state 1, then as time goes by, it

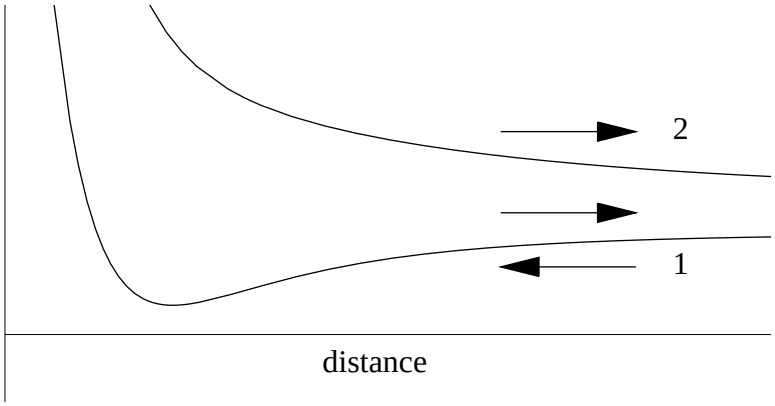

Figure 1.11: Two potentials ('binding' and 'anti-binding') for the relative motion of two atoms.

will also have a nonzero amplitude in state 2, since this amplitude is fed by the other one:

$$\mathrm{i}\hbar\frac{\partial\psi_2(x,t)}{\partial t} = \ldots + V_{21}(x)\psi_1(x,t).$$

It thus happens that in fig.1.11, the particle is incident in state 1 and exits the 'collision' with amplitudes on both states 1 and 2. The problem is to calculate the transition amplitudes towards these two states.

A spin in a magnetic field A particle with spin $\frac{1}{2}$ is a typical example of a system that occurs in two states. In this context, the potential matrix $V(x)$ may be written in terms of a 'scalar potential' $W(x)$ and a 'magnetic field' $\mathbf{B}(x)$. To this end, we introduce the PAULI matrices

$$\begin{aligned}\sigma_1 &= \begin{pmatrix} 0 & 1 \\ 1 & 0 \end{pmatrix} \quad \sigma_2 = \begin{pmatrix} 0 & -\mathrm{i} \\ \mathrm{i} & 0 \end{pmatrix} \\ \sigma_3 &= \begin{pmatrix} 1 & 0 \\ 0 & -1 \end{pmatrix}\end{aligned} \tag{1.60}$$

and write the potential as

$$V(x) = W(x)\mathbf{1} + \sum_i \sigma_i B_i(x) \tag{1.61}$$

where $\mathbf{1}$ is the unit matrix. It is easily shown that the scalar potential and the magnetic field are given in terms of the potential by

$$W(x) = \frac{1}{2}\mathrm{tr}\, V(x) \quad B_i(x) = \frac{1}{2}\mathrm{tr}\ (\sigma_i V(x)) \tag{1.62}$$

In many cases, it is customary to represent the magnetic field as a vector in three-dimensional space. This representation is linked to the behaviour of the 'spin vector' $\boldsymbol{\sigma}$, viewed as a HEISENBERG operator. Indeed, its equation of motion is that of a precessing magnetic moment

$$\boldsymbol{\sigma} = \frac{\mathrm{i}}{\hbar}\,[H, \boldsymbol{\sigma}] = \frac{2}{\hbar}\mathbf{B} \times \boldsymbol{\sigma}$$

with a Larmor frequency $2|\mathbf{B}|/\hbar$. If the 'spin vector' is aligned parallel or antiparallel to the magnetic field vector, no rotation takes place, and the spin is in a (classically) 'stationary' state. These states have an interaction energy $\boldsymbol{\sigma} \cdot \mathbf{B} = \pm|\mathbf{B}||\boldsymbol{\sigma}|$ where the 'magnitude of the spin' has only a precise meaning for a classical magnetic dipole moment.

1.6.3 'Dressed states'

These classical considerations are related to the *eigenstates* of a real spin $\frac{1}{2}$ system. The eigenvalues $A_{1,\,2}$ of the potential matrix are easily shown to be equal to

$$\begin{aligned} &\det \begin{pmatrix} B_3 - A & B_1 - \mathrm{i}B_2 \\ B_1 + \mathrm{i}B_2 & -B_3 - A \end{pmatrix} = 0 \\ &\Longrightarrow \quad A_{1,\,2} = \pm \left(B_1^2 + B_2^2 + B_3^2\right)^{1/2} = \pm|\mathbf{B}| \end{aligned} \tag{1.63}$$

The corresponding eigenstates are calculated in the exercises for the general case. To simplify the calculations, we choose a purely real coupling and put $B_2 = 0$. The eigenstates are then given by

$$\lambda_1 = +|\mathbf{B}|: \quad \Psi_1 = \begin{pmatrix} \cos\vartheta/2 \\ \sin\vartheta/2 \end{pmatrix} \tag{1.64a}$$

$$\lambda_2 = |\mathbf{B}|: \quad \Psi_2 = \begin{pmatrix} -\sin\vartheta/2 \\ \cos\vartheta/2 \end{pmatrix} \tag{1.64b}$$

where ϑ is the angle between the magnetic field vector $B_1\mathbf{e}_1 + B_3\mathbf{e}_3$ and the vector $\mathbf{e}_3$:

$$\tan\vartheta(x) = \frac{B_1(x)}{B_3(x)}. \tag{1.65}$$

The eigenstates (1.64) are also called *'adiabatic'* or *'dressed'* states. The word 'adiabatic' suggests that the magnetic field varies 'slowly' in space such that the moving spin can follow its instantaneous direction. The word 'dressed' refers to spin resonance where the spin eigenstates in a strong vertical field ($B_1 = 0$, no coupling) are 'dressed' by the transverse field B_1 that couples them.

The advantage of the dressed states is that the potential matrix becomes diagonal in this basis. Noting U the unitary transformation that performs the basis change (its columns are the dressed state vectors (1.64)), we have

$$U^\dagger(\boldsymbol{\sigma}\cdot\mathbf{B})U = \Delta = |\mathbf{B}|\sigma_3$$

where the entries of the diagonal matrix Δ are the eigenvalues.

What becomes of the Schrödinger equation in the dressed basis? The magnetic potential has already been dealt with. The scalar potential $W(x)$ is already proportional to the unit matrix and stays so. The time-derivative does not change either because the unitary transformation U does not depend on time. However, since the angle ϑ (1.65) depends on the position x, U varies with x: the dressed basis is only a *'local' basis* and therefore the second derivative transforms into

$$U^\dagger\frac{\partial^2}{\partial x^2}U = \frac{\partial^2}{\partial x^2} + 2U^\dagger\frac{\partial U}{\partial x}\frac{\partial}{\partial x} + U^\dagger\frac{\partial^2 U}{\partial x^2}.$$

A simple calculation therefore gives the following Schrödinger equation

$$\begin{aligned}\mathrm{i}\hbar\frac{\partial\Psi}{\partial t} &= -\frac{\hbar^2}{2m}\left[\frac{\partial^2\Psi}{\partial x^2} - \frac{\mathrm{d}\vartheta}{\mathrm{d}x}\sigma_1\frac{\partial\Psi}{\partial x}\right.\\ &\qquad \left. - \frac{1}{2}\frac{\mathrm{d}^2\vartheta}{\mathrm{d}x^2}\sigma_1\Psi - \left(\frac{1}{2}\frac{\mathrm{d}\vartheta}{\mathrm{d}x}\right)^2\Psi\right] +\\ &\qquad + \left[W(x) + \Delta(x)\right]\Psi(x) \end{aligned} \tag{1.66}$$

where Ψ is now the spinor in the dressed basis (1.64). The last line is the result we wanted to obtain: the potential matrix is diagonal. However, the kinetic energy operator has changed into a weird form: it contains also a off-diagonal potential term proportional to $\mathrm{d}^2\vartheta/\mathrm{d}x^2$ and a first-order derivative with off-diagonal matrix elements.

1.6.4 The adiabatic approximation

The difficulties with the SCHRÖDINGER equation in the adiabatic basis can be overcome when we *simply drop* the terms containing the derivatives of ϑ. The equation then decouples into two scalar equations for the two eigenstates with the potentials $W(x) \pm |\mathbf{B}|$. To give an example, consider a magnetic field of the form

$$B_3 = bx, \quad B_1 = \text{const.} \tag{1.67}$$

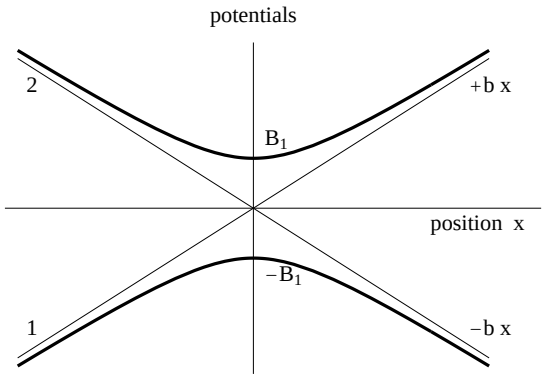

Figure 1.12: Diabatic (thin lines) and adiabatic (thick lines) potentials in a linear level crossing.

The corresponding eigenenergies for $B_1 = 0$ and the dressed energies are shown in fig.1.12. For zero coupling, the potentials are straight lines that cross at $x = 0$. These 'diabatic' (or 'bare') potentials change into two hyperbolae when the coupling B_1 is turned on. The crossing develops into an *'avoided crossing'* and the dressed energies become nondegenerate with a distance of $2B_1$ at $x = 0$.

If there is no coupling, a particle incident from the left in state 1 stays on its potential curve (the SCHRÖDINGER equations decouple!) and exits to the right on the upper curve. (We assume a sufficiently large kinetic energy.) The spin state remains equal to $(1, 0)$ throughout the whole process.

If the coupling is nonzero, however, and the adiabatic approximation holds, the particle will follow the lower dressed level (that connects asymptotically to the incident state 1) and exit for large x on the lower level. During the process, the spin turns its direction and becomes 'spin down' $(0, 1)$ at the end. This may be understood by noting that the magnetic field vector rotates during the process. The relation $\tan\vartheta = B_1/bx$ implies that $\vartheta = \pi$ (field pointing 'downwards') for $x \to -\infty$ and $\vartheta = 0$ (field 'upwards') for $x \to +\infty$ (we assume $B_1 > 0$). At $x = 0$, we have $\vartheta = \pi/2$, the field then points into the x_1 direction (field 'horizontal').

Validity criterion. What arguments may be put forward to justify the adiabatic approximation? The term with the first derivative that we neglect in the Hamiltonian (1.66) is of the order of

$$\frac{\hbar^2}{m}\frac{1}{a}\frac{p}{\hbar} = \frac{\hbar p}{ma}$$

where we have estimated $\mathrm{d}\vartheta/\mathrm{d}x \sim 1/a$ with a the length scale for the variation of the magnetic field, and $\partial\Psi/\partial x \sim p\Psi/\hbar$. This quantity must be small compared to a typical term of the decoupled equations, the kinetic energy, say. This gives the criterion

$$\hbar \ll pa \tag{1.68}$$

that is obviously satisfied if $\hbar$ is sufficiently small. On the other hand, we observe that the adiabatic approximation breaks down when the particle moves too slowly through the avoided crossing. We get the same condition from the second derivative term with the estimate $\mathrm{d}^2\vartheta/\mathrm{d}x^2 \sim 1/a^2$.

One may also have the situation that the (kinetic) energy of the particle is not sufficient to reach the avoided crossing. Then, the turning point is located to the right (for example) of it, and it will turn back in the same diabatic state. If the energy is higher than both adiabatic potentials in the crossing, one may also think of a resonance in the transmitted wave function (on the lower adiabatic potential) due to its coupling to bound states in the upper adiabatic well.

In summary, we see that there must be a cross over in the behaviour of the spin between a rapid and a slow passage through an avoided crossing. In an intermediate region of velocities, one will have nonzero populations on both states. To study this problem in detail, we shall leave the position-dependent SCHRÖDINGER equation (for analytic work on this problem, see Garraway & Suominen (1995)) and study the motion in a frame moving with the particle.

1.6.5 The LANDAU-ZENER level crossing

If we describe the center-of-mass motion classically $x = x(t)$, we still have a SCHRÖDINGER equation for the spinor $\Psi(t)$ that is transported along the classical path:

$$\mathrm{i}\hbar\frac{\mathrm{d}\Psi}{\mathrm{d}t} = \left(W(t) + \boldsymbol{\sigma}\cdot\mathbf{B}(t)\right)\Psi(t) \tag{1.69}$$

where $W(t) = W(x(t))$ etc. The scalar potential can be integrated simply by separating a phase factor $\exp \mathrm{i}\delta(t)$ where $\delta(t)$ is proportional to the integral of $W(t)$. The difficult part is the magnetic potential matrix. We shall suppose again that the coupling field B_1 is real. (The general case gives rise to the BERRY phase discussed in the exercises.)

The LANDAU-ZENER model uses the following magnetic field similar to (1.67)

$$B_3 = \lambda t, \quad B_1 = V = \text{const.} \tag{1.70}$$

The two components of the SCHRÖDINGER equation (1.69) then satisfy the coupled differential equations

$$\begin{array}{rcll} \mathrm{i}\hbar\partial_t\psi_1 & = & \lambda t\psi_1 & +V\psi_2 \\ \mathrm{i}\hbar\partial_t\psi_2 & = & V\psi_1 & -\lambda t\psi_2 \end{array} \tag{1.71}$$

As shown by Zener (1932), these equations have an analytical solution. We eliminate one of the spin components by operating with the derivative $\mathrm{i}\hbar\partial_t$ on the equation for ψ_2:

$$\begin{aligned} -\hbar^2\partial_t^2\psi_2 &= \mathrm{i}\hbar V\partial_t\psi_1 - \mathrm{i}\hbar\lambda\left(1+t\partial_t\right)\psi_2 \\ &= V\left(\lambda t\psi_1 + V\psi_2\right) - \mathrm{i}\hbar\lambda\left(1+t\partial_t\right)\psi_2 \\ &= \lambda^2 t^2\psi_2 + \left(V^2 - \mathrm{i}\hbar\lambda\right)\psi_2 \end{aligned} \tag{1.72}$$

where we have used the differential equations for both $\psi_{1,2}$. We thus find a closed second-order differential equation for ψ_2. This is a parabolic cylinder equation whose standard form is

$$\frac{\mathrm{d}^2\psi}{\mathrm{d}z^2} + \left(\frac{z^2}{4} - a\right)\psi = 0 \tag{1.73}$$

We obtain this form using the dimensionless variables

$$z = \sqrt{\frac{2\lambda}{\hbar}}\,t, \qquad a = -\frac{V^2}{2\hbar\lambda} - \frac{\mathrm{i}}{2}. \tag{1.74}$$

Asymptotic solutions

(*Material not covered in WS 2012/13.*)

We want to find a particular solution of the coupled equations (1.71) according to the following scattering situation: a particle is incident in the state 1 with unit amplitude and exits the crossing region with amplitudes $C_{1,2}$ on the (bare) states 1, 2. The probability of an adiabatic following is then equal to $|C_2|^2$, while $|C_1|^2$ gives the probability that the particle jumps onto the other dressed state (a 'nonadiabatic transition').

We need the asymptotic solutions of (1.71) to fix the form of the incident wave, and in order to identify the amplitudes $C_{1,2}$ of the outgoing waves.

The incident spinor must be of the form

$$\Psi_{\mathrm{inc}}(t\to-\infty) = \begin{pmatrix} \text{const.} \\ 0 \end{pmatrix}$$

with a vanishing amplitude ψ_2. We thus have the boundary condition

$$\psi_2(t \to -\infty) = \psi(z \to -\infty) = 0$$

for the parabolic cylinder equation (1.73).

The outgoing waves may be obtained from the system (1.71) by neglecting the coupling V compared to the 'potentials' $\pm\lambda t$. We thus get

$$\psi_2(t \to \infty) \propto \mathrm{e}^{\mathrm{i}\lambda t^2/2\hbar} = \mathrm{e}^{\mathrm{i}z^2/4} \tag{1.75}$$

and define the coefficient C_2 to be the amplitude in front of this function. If there is a nonzero amplitude on the state 1, a second term enters the asymptotic form of ψ_2. From the differential equation (1.71), we have the relation

$$\psi_1(t) = \frac{1}{V}\left(\mathrm{i}\hbar\partial_t + \lambda t\right)\psi_2$$

We get an outgoing wave $\psi_1 = C_1\mathrm{e}^{-\mathrm{i}\lambda t^2/2\hbar}$ if ψ_2 is of the form

$$\psi_2(t \to \infty) = \frac{VC_1}{2\lambda t}\mathrm{e}^{-\mathrm{i}\lambda t^2/2\hbar}$$

which is subdominant with respect to (1.75). We note that this asymptotic formula also allows to fix the boundary condition for the incident wave: if we write $C_1 = 1$, we get an incident wave on ψ_1 with unit amplitude in the limit $t \to -\infty$.

Translating into the variables for the parabolic cylinder function, we have the following boundary conditions

$$z \to -\infty : \quad \psi(z) = \frac{\sqrt{K}}{z}\mathrm{e}^{-\mathrm{i}z^2/4} \tag{1.76a}$$

$$z \to \infty : \quad \psi(z) = C_1\frac{\sqrt{K}}{z}\mathrm{e}^{-\mathrm{i}z^2/4} + C_2\mathrm{e}^{\mathrm{i}z^2/4} \tag{1.76b}$$

where we have introduced the dimensionless parameter $K = V^2/2\hbar\lambda$.

Analytic solution

According to Abramowitz & Stegun (1972, chap. 19), the two following complex functions are linearly independent solutions to the parabolic cylinder equation (1.73):

$$E(a, z), \quad E^*(a, z) \tag{1.77}$$

Note that these functions are *not* complex conjugates of each other when a is not real. We also get a solution with the replacement $z \mapsto -z$ because the differential equation is even in z. The function $E^*(a, -z)$ is plotted in fig.1.13.

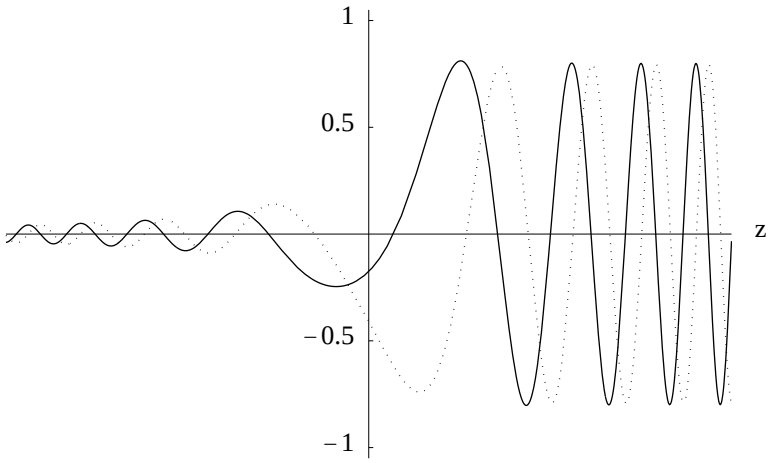

Figure 1.13: Parabolic cylinder function $E^*(a,-z)$ for the LANDAU-ZENER model. Solid line: real part; dotted line: imaginary part. Parameter $a = -1/2\pi + \mathrm{i}/2$.

We need the asymptotic behaviour of these functions in order to compare with our boundary conditions (1.76). For real a, the formulas given in Abramowitz & Stegun (1972, , § 19.21) give

$$z \to +\infty: \quad E(a,z) = \sqrt{\frac{2}{z}}\mathrm{e}^{\mathrm{i}\phi(z)} \tag{1.78a}$$

$$E^*(a,z) = \sqrt{\frac{2}{z}}\mathrm{e}^{-\mathrm{i}\phi(z)} \tag{1.78b}$$

$$\phi(z) = \frac{z^2}{4} - a\log z + \frac{\phi_2}{2} + \frac{\pi}{4} \tag{1.78c}$$

$$\phi_2 = \arg\Gamma(\tfrac{1}{2} + \mathrm{i}a) \tag{1.78d}$$

for z positive and large. In the opposite limit, we get

$$z \to -\infty:$$

$$E(a,z) = -\mathrm{i}\sqrt{\frac{2}{-z}}\left(\mathrm{e}^{\pi a}\mathrm{e}^{\mathrm{i}\phi(-z)} - \sqrt{1+\mathrm{e}^{2\pi a}}\mathrm{e}^{-\mathrm{i}\phi(-z)}\right) \tag{1.79a}$$

$$E^*(a,z) = \mathrm{i}\sqrt{\frac{2}{-z}}\left(\mathrm{e}^{\pi a}\mathrm{e}^{-\mathrm{i}\phi(-z)} - \sqrt{1+\mathrm{e}^{2\pi a}}\mathrm{e}^{\mathrm{i}\phi(-z)}\right) \tag{1.79b}$$

From the comparison with the boundary condition (1.76a), we conclude that $\psi(a,z) \propto E^*(a,-z)$ is the solution we are looking for (see also fig.1.13). Before reading off the coefficients $C_{1,2}$, however, we have to continue analytically the asymptotic formulas to complex values of a. The lonely appearance of $\phi_2 =$

$\arg\Gamma(\frac{1}{2}+\mathrm{i}a)$ is an indication that the expression obtained so far is not yet valid for arbitrary complex a.

To find a formula for complex a, we normalise the solution to an 'incident wave' of the form

$$z\to-\infty:\quad \psi(a,z)=-\frac{N}{\sqrt{-z}}\mathrm{e}^{-\mathrm{i}z^2/4+\mathrm{i}a\log(-z)}$$

including the logarithmic term, with N an overall real constant. Using the identity

$$\left|\Gamma(\tfrac{1}{2}\pm\mathrm{i}a)\right|^2=\frac{\pi}{\cosh\pi a},\qquad a \text{ real},$$

the asymptotics for large and positive z may be written

$$\begin{aligned} &z\to\infty:\\ &\psi(a,z) \;=\; -\frac{N}{\sqrt{z}}\Big(\mathrm{i}\,\mathrm{e}^{\pi a}\,\mathrm{e}^{-\mathrm{i}z^2/4+\mathrm{i}a\log z}+\\ &\qquad\qquad +\frac{\sqrt{2\pi}\,\mathrm{e}^{\pi a/2}}{\Gamma(\frac{1}{2}-\mathrm{i}a)}\,\mathrm{e}^{\mathrm{i}z^2/4-\mathrm{i}a\log z}\Big). \end{aligned} \tag{1.80}$$

This function may now be continued into the complex a plane. In our case, we have $a=-K+\mathrm{i}/2$, and we get

$$z\to-\infty:\quad \psi(z)=\frac{N}{z}\mathrm{e}^{-\mathrm{i}z^2/4-\mathrm{i}K\log(-z)}.$$

An additional factor $(-z)^{-1/2}$ entered from the term $\mathrm{e}^{\mathrm{i}a\log(-z)}$. Apparently, we have to include the logarithmic term into the form of the incident wave. With this modification in the boundary conditions (1.76), we find the normalisation constant $N=\sqrt{K}$. Performing the same modification in the outgoing waves, the asymptotics (1.80) yields the coefficients

$$C_1 \;=\; \mathrm{e}^{-\pi K} \tag{1.81}$$

$$C_2 \;=\; -\frac{\sqrt{2\pi K}}{\Gamma(1+\mathrm{i}K)}\mathrm{e}^{-\pi K/2}\,\mathrm{e}^{\mathrm{i}\pi/4}. \tag{1.82}$$

The behaviour of the probabilities $|\psi_{1,2}(t)|^2$ during the crossing is illustrated in fig.1.14. The probability for state 1 decreases at the expense of state 2. Once the crossing is passed, both probabilities show oscillations that are due to the interference between the two asymptotic terms in (1.76b).

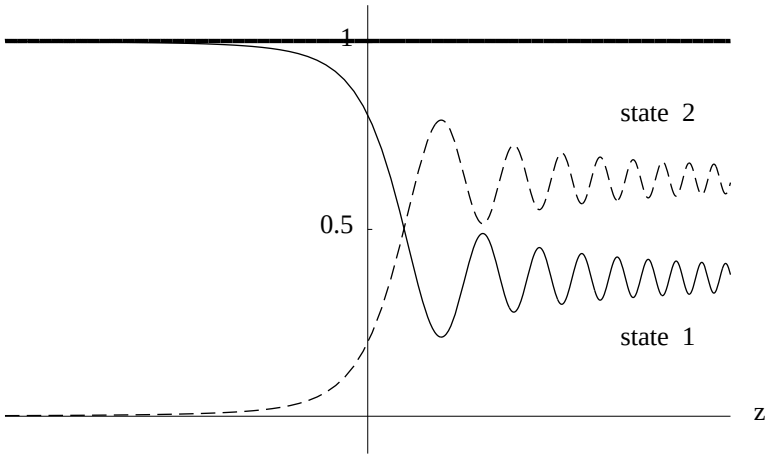

Figure 1.14: Probabilities for the (bare) states 1, 2 in the LANDAU-ZENER model vs. time. The horizontal line shows the sum of the probabilities, equal to one within numerical error. Parameter $K = 1/2\pi$ as in fig.1.13.

Discussion

We started with a particle incident in state 1. From the analytical solution just derived, we can now compute the probability $|C_1|^2$ that the particle stays in that state and the probability $|C_2|^2$ for a state change. The result is

$$|C_1|^2 = \mathrm{e}^{-2\pi K} = \exp\left(-\pi V^2/\hbar\lambda\right) \tag{1.83}$$

$$\begin{aligned} |C_2|^2 &= \frac{2\pi K}{|\Gamma(1+\mathrm{i}K)|^2}\mathrm{e}^{-\pi K} \\ &= 2\mathrm{e}^{-\pi K}\sinh\pi K = 1-\mathrm{e}^{-2\pi K} \end{aligned} \tag{1.84}$$

with the dimensionless parameter $K = V^2/2\hbar\lambda$. If the coupling V is so small that $V^2 \ll \hbar\lambda$, we thus find that the particle stays essentially in its initial state 1. The probability to jump onto the state 2 is of the order of $\pi V^2/\hbar\lambda$. This result being proportional to the square of the coupling strength, it is intuitively clear that it may also be obtained from FERMI's Golden Rule.

The opposite limit of a large coupling corresponds to the semiclassical regime, $\hbar\lambda \ll V^2$. In this limit, the particle changes its state with near certainty. In the adiabatic potential picture, the particle stays on the adiabatic potential that connects to its initial state. This is shown in fig. 1.15, where the probabilities for the adiabatic (or dressed) states are plotted as a function of time. One observes a much smoother behaviour (without oscillations). Due to the nonadiabatic transition, the probability for the lower dressed state does not stay constant. In the adiabatic basis, it appears that the nonadiabatic transition

happens quite smoothly, shortly after the passage through the level crossing. We observe that the crossover to the adiabatic behaviour occurs for a coupling

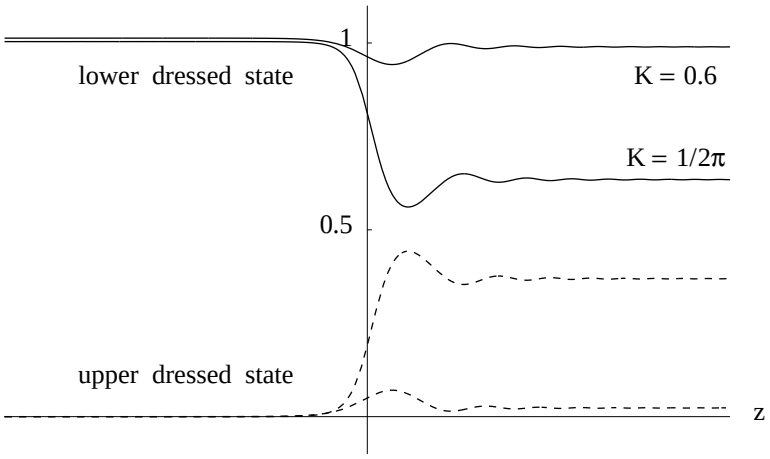

Figure 1.15: Probabilities for the dressed states (upper and lower dressed level in fig.1.12) vs. time. The middle curves show the case $K = 1/2\pi$ as in fig.1.13. The top and bottom curves correspond to $K = 0.6$, the behaviour is nearly fully adiabatic.

strength of the order of $V \sim \sqrt{\hbar\lambda/\pi}$. The dressed state probabilities are then approximately constant in time.

Restore motion. We can translate the results obtained for the time-dependent Landau-Zener model into a level crossing in real space. One has to assume that the velocity p/m is constant during the process. The difference in energy between the two potentials may be written in terms of a 'force' F,

$$V_1(x) - V_2(x) \approx -2F(x - x_c).$$

In the frame moving with the particle, the energy difference is then $-2Fp(t - t_c)/m$, and hence the parameter $\lambda = |F|p/m$. Noting again B_1 the coupling between the two 'bare' potentials, the probability of following adiabatically the dressed state potential is equal to

$$w_{\rm ad} = 1 - \exp\left(-\pi m B_1^2/(\hbar|F|p)\right) \tag{1.85}$$

This probability is essentially unity when p is smaller than the critical momentum $p_{cr} = \pi m B_1^2/(\hbar|F|)$. However, our picture of a particle with a fixed classical trajectory breaks down when the wavelength becomes comparable with

the 'size' $\sim |B_1/F|$ of the crossing region. In the framework of the time-dependent LANDAU-ZENER theory, adiabatic following therefore holds in the following 'window' of momenta

$$\frac{\hbar|F|}{|B_1|} \ll p \ll \frac{\pi m B_1^2}{\hbar|F|}$$

If the left inequality is violated, one has to solve the space-dependent bi-potential problem. If the right inequality is violated, the particle moves too rapidly through the crossing and its spin cannot follow the magnetic field. The particle then changes onto the other adiabatic potential.

Example

The LANDAU-ZENER model is being used in numerous and very different problems. We simply one example from molecular physics.

Light-assisted collisions. In molecular physics, one may study light-assisted collisions between two atoms. The atom pair exists in two states: both atoms in the ground state or an ground-state excited-state pair. In the excited state, the

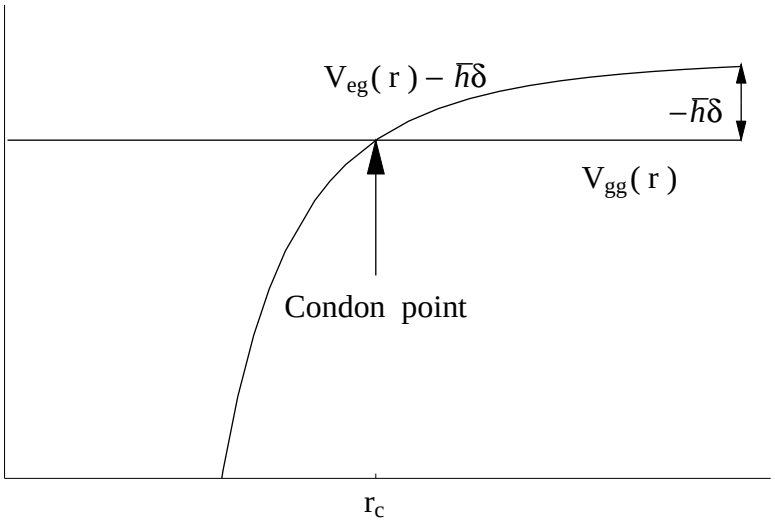

Figure 1.16: Potentials between pairs of atoms.

electronic wave function is different and has a larger energy. This also changes the interaction energy between the atoms. In the so-called BORN-OPPENHEIMER approximation, one assumes that the electronic wave function adapts itself to

the instantaneous positions of the nuclei much faster than the timescale of the nuclear motion. One then gets a potential matrix of the form

$$V(r,t) = \begin{pmatrix} V_{gg}(r) & -\mathbf{d}\cdot\mathbf{E}(t) \\ -\mathbf{d}\cdot\mathbf{E}(t) & \hbar\omega_e + V_{eg}(r) \end{pmatrix}$$

where $\hbar\omega_e$ is the energy of an isolated excited atom, r is the relative distance, $\mathbf{d}$ the electric dipole matrix element and $\mathbf{E}(t)$ the electric field of the light.

This potential matrix is explicitly time-dependent via the light field. We can get back to a time-independent coupling using the *'rotating wave approximation'*. To this end, we introduce modified wave functions (the 'rotating frame')

$$\begin{aligned} \psi_{gg}(r,t) &= \tilde{\psi}_{gg}(r,t) \\ \psi_{eg}(r,t) &= \mathrm{e}^{-\mathrm{i}\omega t}\tilde{\psi}_{eg}(r,t) \end{aligned}$$

with ω a yet undetermined frequency. From the SCHRÖDINGER equation, we find the following equation of motion for the modified amplitudes

$$\begin{aligned} \mathrm{i}\hbar\partial_t\tilde{\psi}_{gg}(r,t) &= V_{gg}(r)\tilde{\psi}_{gg}(r,t) - \mathrm{e}^{-\mathrm{i}\omega t}\mathbf{d}\cdot\mathbf{E}(t)\tilde{\psi}_{eg}(r,t) \\ \mathrm{i}\hbar\partial_t\tilde{\psi}_{eg}(r,t) &= -\mathrm{e}^{\mathrm{i}\omega t}\mathbf{d}\cdot\mathbf{E}(t)\tilde{\psi}_{gg}(r,t) - (\hbar\delta - V_{eg}(r))\,\tilde{\psi}_{eg}(r,t) \end{aligned}$$

where the *'detuning'* is the difference $\delta = \omega - \omega_e$. We now assume that the light field is monochromatic and choose its frequency equal to ω. This gives

$$\mathrm{e}^{\mathrm{i}\omega t}\mathbf{E}(t) = \mathrm{e}^{\mathrm{i}\omega t}\left(\mathbf{E}\,\mathrm{e}^{-\mathrm{i}\omega t} + \mathbf{E}^*\mathrm{e}^{\mathrm{i}\omega t}\right) = \mathbf{E} + \mathbf{E}^*\mathrm{e}^{2\mathrm{i}\omega t}$$

The rotating wave approximation consists in neglecting the oscillating exponential in this expression. This is justified when the time scales involved in the differential equation are much longer than the period $2\pi/\omega$ of the laser field. One may then replace the coupling terms by their average over one field period. We thus get the following potential matrix in the rotating frame:

$$\tilde{V}(r) = \begin{pmatrix} V_{gg}(r) & -\mathbf{d}\cdot\mathbf{E}^* \\ -\mathbf{d}\cdot\mathbf{E} & -\hbar\delta + V_{eg}(r) \end{pmatrix}$$

that is now time-independent.

The ground state potential $V_{gg}(r)$ typically behaves as a $-1/r^6$ power law at large distance. At sufficiently large distances, it becomes negligible compared to the excited-ground state potential $V_{eg}(r) = -C_3/r^3$. If the detuning is negative, one thus gets a level crossing at the position $r_c = (-\hbar\delta/C_3)^{1/3}$ (see fig.1.16). This position is also called the 'CONDON point'. Linearizing the potentials around the crossing point r_c, we get the parameter $\lambda = 3C_3v_c/2r_c^4$ where

v_c is the relative velocity of the atom pair. The light coupling is conveniently written in terms of a RABI frequency $\hbar\Omega = |\mathbf{d} \cdot \mathbf{E}|$. The LANDAU-ZENER model thus gives the following expression for the probability that the atom pair will jump onto the excited-ground state potential (the 'excitation probability')

$$P_{\text{exc}} = 1 - \exp\left(-2\pi\hbar\Omega^2 r_c^4 / 3C_3 v_c\right)$$

see Mastwijk & al. (1998). From this expression, we can get the rate for the creation of ground-excited atom pairs by multiplying with the number of atom pairs per unit time, $4\pi r_c^2\, n\, v_c$, that cross the CONDON point (n is the atomic number density). One also has to average this rate over the atomic velocity distribution. Finally, in the reference given above, the atoms that underwent the excitation are detected because they ionize when they collide on the inner part of the $V_{eg}(r)$ potential.

Bibliography

M. Abramowitz & I. A. Stegun, editors (1972). *Handbook of Mathematical Functions*. Dover Publications, Inc., New York, ninth edition.

M. V. Berry & K. E. Mount (1972). Semiclassical approximations in wave mechanics, *Rep. Prog. Phys.* **35**, 315–397.

M. Born & E. Wolf (1959). *Principles of Optics*. Pergamon Press, Oxford, 6th edition.

N. Fröman & P. O. Fröman (1965). *JWKB approximations: contributions to the theory*. North-Holland, Amsterdam.

B. M. Garraway & K.-A. Suominen (1995). Wave-packet dynamics: new physics and chemistry in femto-time, *Rep. Prog. Phys.* **58**, 365–419.

R. E. Langer (1937). On the connection formulas and the solutions of the wave equation, *Phys. Rev.* **51**, 669–76.

H. C. Mastwijk, J. W. Thomsen, P. van der Straten & A. Niehaus (1998). Optical collisions of cold, metastable helium atoms, *Phys. Rev. Lett.* **80**, 5516–19.

A. Messiah (1995). *Mécanique quantique*, volume I. Dunod, Paris, nouvelle edition.

E. Schrödinger (1926). Quantisierung als Eigenwertproblem. I, *Ann. Phys. (IV)* **79**, 361–376.

H. Wallis, J. Dalibard & C. Cohen-Tannoudji (1992). Trapping atoms in a gravitational cavity, *Appl. Phys. B* **54**, 407–419.

C. Zener (1932). Non-adiabatic crossing of energy levels, *Proc. R. Soc. London A* **137**, 696–702.